Final Report

PROBABILITY DISTRIBUTIONS OF PRECIPITATION-SCATTER INTERFERENCE

By: ROY H. BLACKMER, JR.

Prepared for:

NATIONAL AERONAUTICS AND SPACE ADMINISTRATION
OFFICE OF RESEARCH GRANTS AND CONTRACTS
CODE SC
WASHINGTON, D.C. 20546

CONTRACT NASr-49(23)

STANFORD RESEARCH INSTITUTE

MENLO PARK, CALIFORNIA

STANFORD RESEARCH INSTITUTE
MENLO PARK CALIFORNIA

April 1966

Final Report

PROBABILITY DISTRIBUTIONS OF PRECIPITATION-SCATTER INTERFERENCE

Prepared for:

NATIONAL AERONAUTICS AND SPACE ADMINISTRATION
OFFICE OF RESEARCH GRANTS AND CONTRACTS
CODE SC
WASHINGTON, D.C. 20546

CONTRACT NASr-49(23)

By: ROY H. BLACKMER, JR.

SRI Project 5372

Approved: M. G. H. LIGDA, MANAGER
AEROPHYSICS LABORATORY

D. R. SCHEUCH, EXECUTIVE DIRECTOR
ELECTRONICS AND RADIO SCIENCES

Copy No. 4

ABSTRACT

Meteorological data at and in the vicinity of Portland, Maine, have been analyzed to assess the probability distributions of radio interference received via forward scatter of radiation by precipitation. This precipitation-scatter interference has been expressed in terms of an effective interference temperature for comparison with magnitudes of sky temperature and receiver noise temperatures. It was found that with a standardized value of interfering power of one picowatt per square meter per cycle per second, values of interference temperature could be as high as 10^5K. Probability distributions, by season, of various magnitudes of interference temperature are presented both for the condition in which the interfering signal is present at all altitudes and that in which it is only present above various specific altitudes.

A comparison is made between the probability distributions of interference temperature and the probable values of sky temperature. In these comparisons it is shown that during periods of precipitation the sky temperature increases less rapidly with rainfall rate than does interference temperature. As a result, for very short periods of time the interference temperature greatly exceeds the sky temperature.

The report shows relationships between precipitation and probable interference temperature that may be used to interpret the results at Portland, Maine, in terms of seasonal distribution and vertical extent of precipitation, at other locations.

Author

CONTENTS

ILLUSTRATIONS

TABLES

I INTRODUCTION, SUMMARY, AND CONCLUSIONS

A. INTRODUCTION

Dennis[1]* pointed out the importance of precipitation-scatter of SHF radio waves as a source of interference. Experiments conducted by Stanford Research Institute[2] and the Central Propagation Laboratory of the National Bureau of Standards[3] confirmed the reality of precipitation-scatter as a potential interference mode. A realistic assessment of the importance of this interference at any receiver site requires a consideration of its probability distribution with time.

The basic theory of forward scatter of electromagnetic radiation by precipitation has received considerable attention over a period of many years, therefore the important precipitation-scatter parameters are well known. The parameters of primary importance are the particle size distributions and the state (liquid or ice) of the precipitation particles and their variation over the path along which an antenna is looking. No direct measurements of particle size distributions exist in sufficient detail for direct determination of probability distributions. It is therefore necessary to find methods of estimating probable particle size distributions along extended paths from other types of data that are routinely collected and for which a sufficient period of record exists to specify a probability distribution.

A source of pertinent data is the observations of the duration, intensity, and type of precipitation made routinely at numerous U.S. Weather Bureau stations for many decades. Relationships between the intensity of precipitation at the surface and the vertical profile of precipitation particles have been deduced from radar observations. The radar studies include (1) studies of relatively uniform widespread

---

*References are listed at the end of the report.

precipitation within which there is a well-marked transition between raindrops at low levels and snow crystals at the higher altitudes and (2) studies primarily of the more intense but localized convective precipitation, such as that associated with thunderstorms. The latter studies provide knowledge of variations in precipitations both in the vertical and in the horizontal from the edges to the center of the storm.

This report shows how available data may be treated to arrive at probability distributions of precipitation-scatter interference for Portland, Maine. Specifically, the report deals with the following tasks as given in the contractual statement of work:*

"(1) Derive the probability distribution of the effective interference temperature,† T_i, due to precipitation scatter with a standardized flux of interfering power at a frequency of 6 Gc above various specified heights, for a selected station in the northeastern United States, as a function of angular elevation, season, and time of day.

"(2) Compare this with the probable values of the sky temperature, T_s, to determine the maximum values of interfering power flux that could be permitted under various conditions without producing significant increases in interference in a low-noise receiver.

"(3) To present the results of (1) and (2) above in general form suitable for use in predicting the probability of interference in ground satellite stations from other terrestrial stations, and vice versa, by correlating (a) meteorological data; (b) site parameters, both physical and electrical; (c) the effects of intervening

---

*See Statement of Work under Contract NASr-49(23).

†The concept of expressing precipitation scatter in terms of an interference temperature is discussed in Section IIA.

terrain; and to recommend criteria to minimize or eliminate the interference due to precipitation scattering."

Task (1) specifies a selected station in the northeastern United States. This area was chosen because it is well covered by weather radars and has many reporting weather stations. Furthermore, the U.S. terminal for the TELSTAR satellites is located there, so that the results would have some immediate application. To this end, data from Portland, Maine, have been utilized extensively in this study.

B. SUMMARY

Forward scatter of radiation from a distant transmitter into the antenna beam of a receiver due to precipitation in the common volume has been recognized as a source of potential interference in communications. This precipitation-scatter interference has been expressed in terms of an interference temperature, and the important precipitation parameters have been defined. Models were constructed using the results of available radar studies to relate surface precipitation rates to the horizontal and vertical precipitation intensity profiles with a given surface rainfall rate. Based on these models and data on observed rainfall as recorded by U.S. Weather Bureau observers at Portland, Maine, and radar data from MIT (Cambridge, Massachusetts), probability distributions of interference temperatures that could be expected in the New England area were prepared.

The probability distributions of interference temperature were prepared for each season of the year with the assumption that the interfering signal was present above various specific levels. These interference temperatures were compared with expected sky temperatures.

Also, a comparison was made of probable interference temperatures at other potential sites with those at Portland, Maine. This comparison was based on the seasonal distribution of precipitation and the probable vertical extent of precipitation at other locations.

C. CONCLUSIONS

With the assumption of an interfering signal of one picowatt per square meter per cycle per second, it was found that interference temperatures at Portland, Maine, would range from 10^0K to 10^6K. The lower value would be exceeded several days per month during all seasons of the year, while the higher value would be exceeded only about 5 minutes during the summer and fall months, when the antenna elevation angle was close to the horizon and the interfering signal was present at all levels. When the interfering signal was only present above relatively high levels, the interference temperature was nonexistent. The critical levels were: winter, 6 km; spring, 8 km; summer, 14 km; and fall, 8 km.

Comparison of interference temperatures and sky temperatures showed that several days each month of each season the former will exceed the latter. As increasingly shorter time periods are considered, the interference temperatures greatly exceed the sky temperatures. For example, sky temperatures probably would not exceed 10^3K even at low elevation angles during intense thunderstorms in July, while interference temperatures could exceed 10^6K.

Comparison of the climatology of other areas with that at Portland, Maine, shows that there are areas that would have quite different probability distributions of interference temperature. Some parts of the United States, notably the north central Midwest, have very little wintertime precipitation, and up to 30 percent of the annual precipitation may be in the form of snow, which will produce very low interference temperatures. Other areas, e.g., the Pacific Coast region, have practically no summertime precipitation and therefore would have very little precipitation-scatter interference during the warmer half-year. The maximum precipitation-scatter interference would be in locations like the Gulf Coast area of the United States, where there is much precipitation each month and the majority of this precipitation is of the convective type, extending to quite high altitudes since the area has a high tropical tropopause.

Additional studies are required, especially those utilizing quantitative radar data at a number of locations, for a more accurate description of the three-dimensional distribution of precipitation.

II DETERMINATION OF MAGNITUDES OF PRECIPITATION-SCATTER INTERFERENCE

A. PRECIPITATION SCATTER AS AN INTERFERENCE TEMPERATURE

For consideration of the problem of precipitation scatter it has been found useful to introduce the concept of an effective interference temperature, T_i, defined according to

$$P_i = k\, T_i\, B \quad , \tag{1}$$

where P_i is the mean power level of the interfering signal, k is Boltzmann's constant, and B is the bandwidth of the interfering signal. Interference temperature T_i is directly comparable to T_n, the receiver noise temperature, and T_s, the sky temperature, which ordinarily are used to specify the performance of sensitive receiver systems.

Consider a receiving antenna with a narrow uniform beam directed into an array of precipitation particles scattering isotropically with cross section η per unit volume and illuminated by uniform radiation of intensity p' per unit area per unit bandwidth. The received interfering power is given by

$$P_i = \frac{p' B \lambda^2}{4\pi} \int_o^\infty \eta \, dl \quad , \tag{2}$$

where λ is the wavelength and l denotes distance along the beam.

By combining Eqs. (1) and (2), one can write

$$T_i = \frac{p' \lambda^2}{4\pi k} \int_o^\infty \eta \, dl \quad . \tag{3}$$

The presence of λ^2 in the numerator of Eq. (3) does not mean that T_i decreases with frequency, since η is also frequency-dependent. In the Rayleigh region, η varies as the fourth power of the frequency--i.e., as λ^{-4}.

It is useful to assume a standard value of p' to derive a standardized T_i. A convenient value for p' is 10^{-12} Watts m^{-2} sec (1 picowatt per square meter per cycle per second). With this standard value of interfering power and a wavelength of 5 cm, Eq. (3) becomes

$$T_i = 1.44 \times 10^7 \int_o^\infty \eta \, dl \quad . \tag{4}$$

The solution of this equation requires the distribution of η along the antenna path. This distribution will depend on the type and intensity of the precipitation.

Meteorologists generally divide precipitation into two categories: (1) the widespread, relatively continuous stratiform type of precipitation wherein large areas experience roughly the same precipitation over relatively long time periods; and (2) localized convective precipitation that brings brief scattered showers for relatively short periods of time. These two types are distinctly different in their precipitation-scatter effects because of unique distributions of particle size and state of water. The continuous precipitation is generally less intense and has a well-marked transition between liquid water at low levels and frozen water at the higher levels. Convective precipitation has variations in particle size distribution, both in the horizontal and the vertical, that must be considered. Available studies of these two types of precipitation have been examined and useful material summarized to formulate models of the scattering cross sections of continuous and convective precipitation.

B. CONTINUOUS PRECIPITATION

1. Scattering Cross Sections

To evaluate the term ηdl given in Eq. (4) it is necessary to know the vertical extent of the precipitating column and the variations of η with altitude. A number of radar measurements of vertical profiles of reflectivity in continuous precipitation have been made. Figure 1 shows 18 profiles presented by Wexler and Austin.[4] These profiles have been superimposed about the 0° isotherm, since the profiles would be expected to show major discontinuities at this level. The profiles

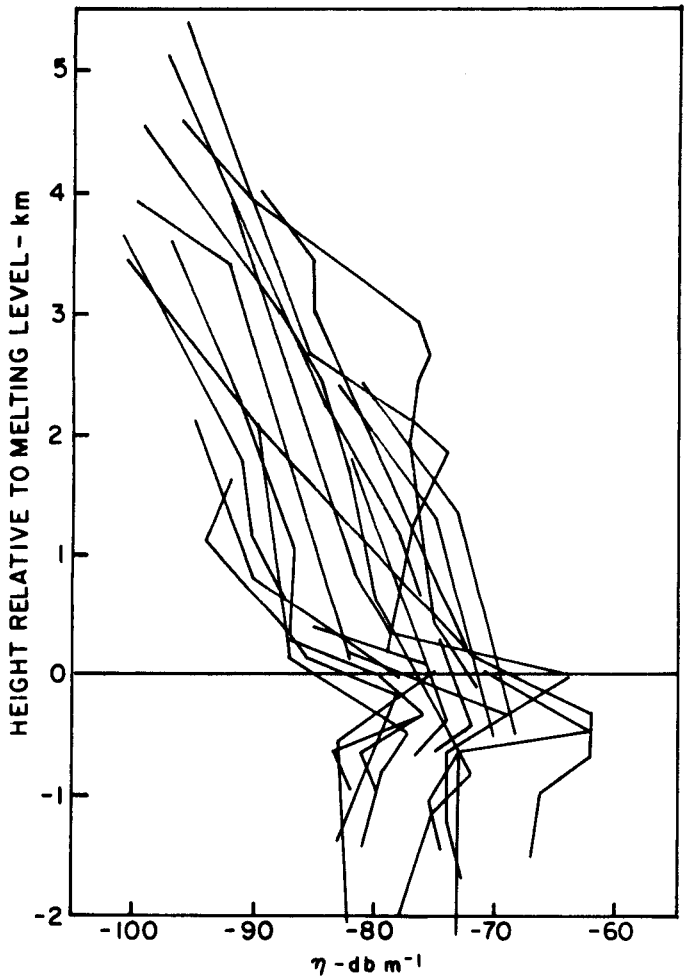

FIG. 1 VERTICAL PROFILES OF BACKSCATTERING CROSS SECTIONS OF CONTINUOUS PRECIPITATION (After Wexler and Austin, Ref. 4)

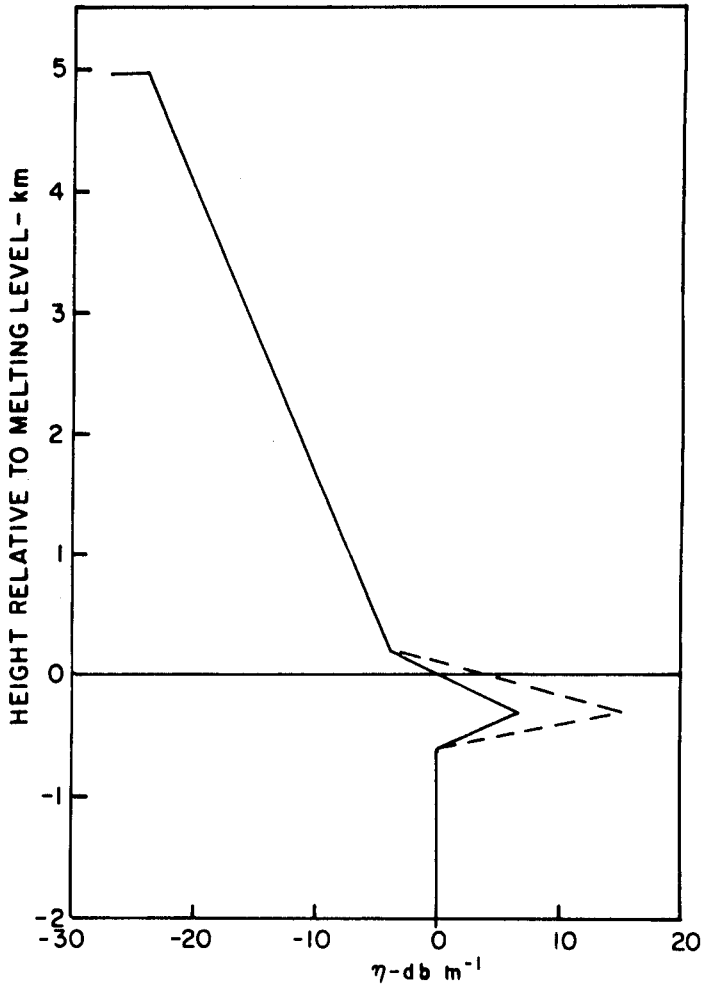

FIG. 2 MODEL PROFILE OF BACKSCATTERING CROSS SECTION OF CONTINUOUS PRECIPITATION

show some variations, but there is a consistency evident in the shapes with basically only a horizontal displacement dependent on rainfall rate. Figure 2 is a model reflectivity profile derived from the curves in Fig. 1. This model has several characteristics that are worth mentioning. First, the reflectivity is uniform up to an altitude just below the 0° isotherm. Second, there is an increase in reflectivity through the melting layer (the so-called radar bright band) where water-coated snowflakes scatter more strongly than either raindrops or snow crystals. Finally, there is a uniform decrease in reflectivity for an altitude interval of some 5 km above the melting level. This model of the backscatter cross section in and above the melting level relative to that in the rain below the bright band is quite useful, in that the backscatter from the rain can in turn be related to the surface rainfall rate. The relationship given by Dennis[5] is

$$\eta = 6.9 \times 10^{-12} f^4 R^{1.6} \quad , \tag{5}$$

where

η = backscattering cross section per unit volume (m^{-1})

f = frequency in Gc

R = rainfall rate in mm hr^{-1}

at $f = 6$ Gc

then $\eta = 8.94 \times 10^{-9} R^{1.6}$.

Relationships between surface rainfall rates and radar reflectivity in the lowest scattering volume have been tested by Austin,[6] who found good agreement if a two-minute time lag was allowed.

One complication which arises in the problem of deducing forward scattering models from radar backscattering cross sections is the enhanced forward scatter in the region of the bright band. In the bright band, where large nonspherical water-covered snowflakes exist,

scattering varies widely with scattering angle.[2] The dashed curve in Fig. 2 represents the increase in the forward direction. Both curves in Fig. 2 are for the case wherein the receiving antenna's polarization in aligned with that of the interfering source.

The reduction due to cross-polarization will depend on the relative numbers of Rayleigh and Mie-type scatterers. For perfectly spherical Rayleight scatters there would be no received cross-polarized signal. The bright band, however, consists of relatively large non-spherical Mie particles which will depolarize the radio waves incident on them. As a result, a cross-polarized component of the scattered signal will still be present. This cross-polarized signal was shown by Fernald and Dennis[7] to be 10 to 25 dB below the signal that would be present with like polarization if the angle between the transmitter and receiver were very large (close to 180 degrees).

To convert from the model of backscattering cross section shown in Fig. 2 to interference temperatures requires, as noted previously, knowledge of the surface rainfall rate. Figure 3 shows magnitudes of interference temperature that would be expected due to radiation from an interference source of one picowatt per square meter per cycle per second incident on the precipitation scatterers in the receiving antenna beam above the level indicated on the ordinate. Two specific conditions are presented: (1) a vertically pointing receiving antenna (solid curve), where the scattering is at an angle of approximately 90 degrees with respect to the interference source over the horizon; and (2) a receiving antenna looking at an elevation angle of 10 degrees above the horizon in the direction of the interference source (dashed curve) where scattering will be in the forward direction at an angle of approximately 170 degrees. Thus, for a given precipitation rate, the interference temperature for the second condition is increased due to enhanced scattering in the forward direction as well as to the longer path through the precipitation at this lower elevation angle. The figure shows that with even relatively low rainfall rates and a depth of precipitation of 4 km below the melting level, interference temperatures exceed many hundreds of degrees Kelvin.

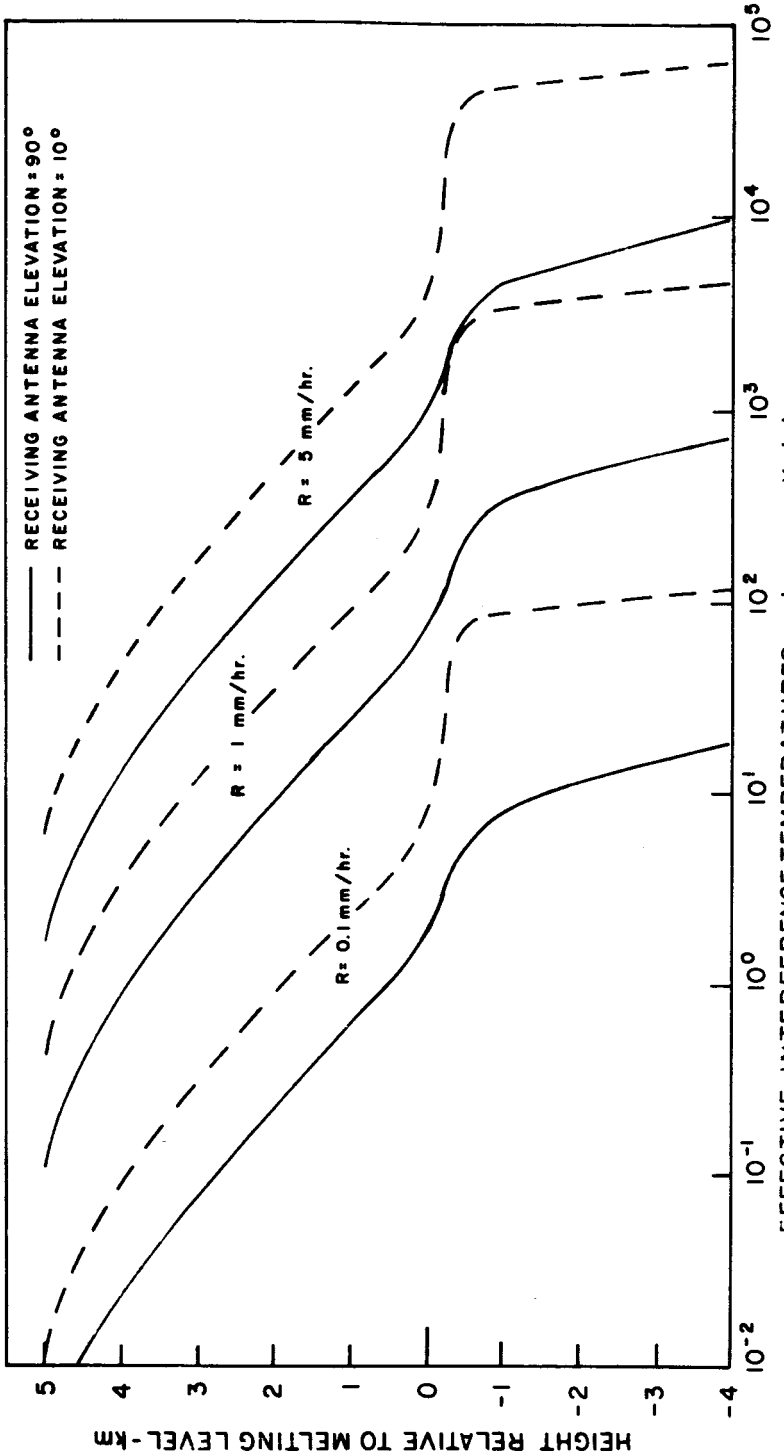

FIG. 3 RELATIONSHIP BETWEEN PRECIPITATION INTENSITY, HEIGHT OF MELTING LEVEL, AND INTERFERENCE TEMPERATURE

The frequencies at which various combinations of rainfall rates and heights of melting levels obtain are discussed below.

2. Frequency

To use the model of interference temperatures from continuous precipitation, it is necessary to know the intensity of surface precipitation and the height of the melting level. These two items are available in weather records for many weather stations around the globe. In this study, data for Portland, Maine, were examined to extract the required information. First, weather observations recorded on U.S. Weather Bureau Form WBAN-10B (available on microfilm) for the months of January, April, July, and October for the years 1957 to 1961 were obtained. These forms contain observations of the time to the nearest minute that various types and intensities of precipitation began or ended. One limitation is that intensities are in broad intervals designated as light, moderate, or heavy. The limits of the intensity intervals for several types of precipitation are given in Table I.

Table I

PRECIPITATION RATES IN

VARIOUS REPORTED INTENSITY INTERVALS

Reported Rainfall Intensity	mm/hr^{-1}
Light	Trace - 2.5
Moderate	2.9 - 7.6
Heavy	>7.6

The vertical temperature profile, together with relative humidity, is measured twice daily by balloon-borne radiosondes. From these profiles the height of the zero-degree isotherm, and hence the melting level, can be extracted. Data on the durations of various intensities of rainfall associated with various melting-level altitudes were extracted from the microfilm for the months and years mentioned above and were tabulated in the following form:

$$TT\ M_L M_L\ ttt\ i$$

where

TT = the hour of the day

$M_L M_L$ = the altitude of the melting level

ttt = the duration in minutes

i = the intensity interval.

This information was placed on punch cards for computer processing. The computer was also given the data from Fig. 3 in tabular form. Thus, the actual height and intensity of precipitation could be compared with the model and an interference temperature computed for each set of conditions.

C. CONVECTIVE PRECIPITATION

1. Scattering Cross Sections

The convective type of precipitation is by definition discontinuous in horizontal extent. The precipitating columns, or convective cells, consist of a central core of more intense rainfall with a rainfall gradient from the maximum value at the center to a value of zero at the edge of the cloud. Not all of the convective cells are necessarily of the same depth over an area, and cells form, grow to some maximum size, and then dissipate. At any given time, therefore, there will be cells of various sizes and stages of development over an area, and each cell will have a different vertical and horizontal profile of reflectivity. A model must, therefore, be expressed in terms of cell dimensions. Fortunately, there is some relationship between the horizontal and vertical extent of convective cells. Byers and Braham[8] found that the diameter was equal to the height of the smaller cells. When the convective area exceeds a certain threshhold, the relationship is no longer valid, because altitudes of tops above, say 23 km, would probably never occur, and this would correspond to a diameter of about 22 km. Actual diameters of convective precipitation (containing many individual cells) of many tens of kilometers are not uncommon.

The model relating diameter and height that has been assumed for convective precipitation is shown in Fig. 4. According to this model, diameter is equal to height up to a value of about 15 km. Then, as the diameter increases to about 20 km, the height drops to about 9 km; thereafter, for any path length through the precipitation the height remains constant at 9 km. Although this model may seem somewhat arbitrary, there are valid reasons for our acceptance of it.

First, as discussed above, there is an established relationship between diameter and height up to a point. Second, studies by Hanks[9] et al and Long[10] have shown that there is some limited penetration of the tropopause* by the more severe (larger) thunderstorms. Thus, a model allowing tops of the larger-diameter convective cells to extend above the mean tropopause (shown on Fig. 4 at about 11.5 km) agrees with observations. Finally, the less severe convective activity (i.e., more widespread), as recognized by the lack of individual sharply defined cells, could reasonably be expected not to reach the tropopause level. Our choice of a hight some 2-1/2 km below the tropopause for the widespread convective activity could probably be verified by a detailed study of radar vertical cross sections.

With this assumed relationship between horizontal and vertical dimensions, the additional information required to evaluate $\int \eta dl$ is the variations of η along any path 1 through the convective precipitation.

Dennis[11] expressed the horizontal variation of reflectivity through the core of a cylindrical model shower as

$$Z' = c(r_o - r)^{2.5} \quad , \tag{6}$$

*see Sec. VB2 for a discussion of the vertical extent of convective precipitation relative to the tropopause.

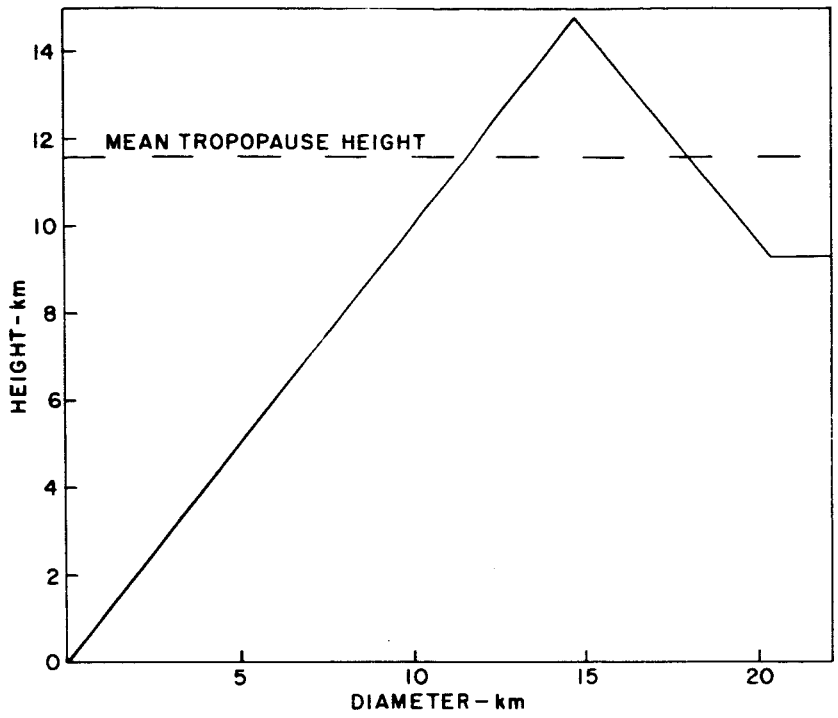

FIG. 4 RELATIONSHIP BETWEEN HORIZONTAL AND VERTICAL EXTENT OF CONVECTIVE PRECIPITATION

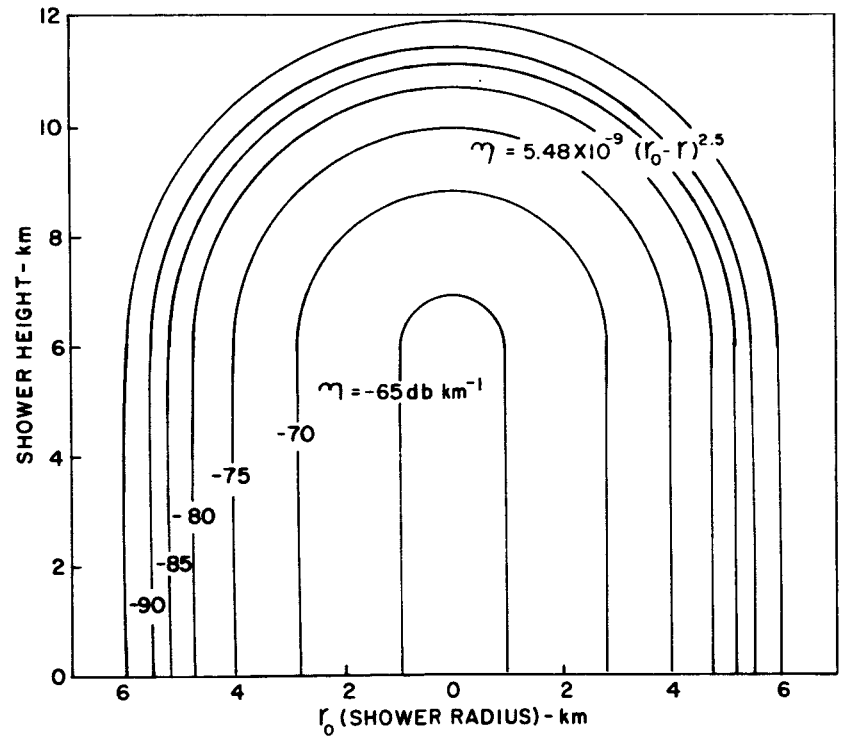

FIG. 5 HORIZONTAL AND VERTICAL VARIATIONS OF BACKSCATTERING CROSS SECTION OF A SHOWER

where

Z' = equivalent radar reflectivity

r_o = shower radius

r = distance from center of shower.

At a frequency of 6 Gc, the backscattering cross section per unit volume is then

$$\eta = 4.57 \times 10^{-8} Z' = 4.57 \times 10^{-8} c(r_o - r)^{2.5} \quad . \qquad (7)$$

This model was extended to cover the vertical profiles of η. The lower half of the shower was assumed cylindrical, with η varying radially as in Eq. (6), and the upper half was assumed to be dome shaped, with η again varying radially as in Eq. (6) (see Fig. 5).

In the simplest example, where interference results from scattering along the entire path horizontally through the lower half of the shower, substitution of Eq. (7) into Eq. (4) gives

$$T_i = 1.44 \times 10^7 \int_{r_o}^{o} 4.57 \times 10^{-8} c(r_o - r)^{2.5} dl \qquad (8)$$

$$T_i = 0.376\ c r_o^{3.5} \quad .$$

Dennis[11] found that $c = 120$ fits quite well the reflectivity values within showers in tropical air masses, regardless of geographical location. For cases where the height of the shower, H, is assumed equal to the diameter of the shower, L,

$$T_i = 4.05\ H^{3.5} \quad . \qquad (9)$$

To account for longer paths through showers where $L > H$, the above expression is multiplied by the ratio L/H, giving the basic expression

for the interference temperature from showers of

$$T_i = 4.05\ H^{2.5} L \quad . \tag{10}$$

To account for the variety of situations which do occur, such as path lengths through the dome of the shower where η no longer varies as in Eq. (7), or when only a fraction of the total pathlength through the shower is contributing noise, the basic expression, Eq. (1), must be modified. This is given in detail in the appendix.

2. Frequency

Convective precipitation presented much more of a problem than continuous precipitation. Continuous precipitation lasts many hours at a given site, so that the short time a large area was approaching or retreating from the station was negligible compared to the time it was over the station. With convective precipitation, numerous cells could be in the vicinity of the site, and the time cells actually over the site would be very small compared to the time cells within interfering range. Thus, data collected at a given location where the weather observer records only what is happening over his rain gage do not adequately describe the true picture of convective activity. To solve the problem of the frequency with which convective precipitation might be within an area but not over a specific site, radar data were examined. These radar data, collected at a site in the New England area, showed the distribution and horizontal dimensions of all precipitation areas within a radius of the station that varied according to the range at which the display was being photographed. The data examined were from the SCR/615-B and AN/CPS-9 radars at MIT in Cambridge, Massachusetts. The wavelengths of the two sets are 10 and 3.2 cm (3 and 0.2 Gc), respectively. Generally, the photographed range was 120 nm, and the input to the photographed scope was from the SCR-615-B. On a few occasions, however, the CPS-9 display was photographed on ranges out to 400 statute miles.

The method of selecting and analyzing specific PPI photographs was as follows. The available radar data were examined, and the times and durations of periods when shower-type precipitation was on the radarscope were tabulated. From this tabulation, photographs were chosen for each of four daily time periods for each month for which data existed, from the months May, June, July, and August in the years 1952, 1953, and 1955. Each selected photograph was examined at 10 randomly selected azimuths. These azimuths were selected by dividing the circle surrounding the station into three 120 degree sectors with boundaries at 060, 180, and 300 degrees. Two azimuths were selected in the 060-to-180-degree sector, and four each from the remaining two sectors. This weighting was made because the 060-to-180-degree sector is primarily over water, where shower behavior would be different than over land. The azimuths were generated by sequentially selecting three-digit numbers from a table of random numbers, multiplying each number by 0.120 and adding it to the initial angular value of the sector within which the azimuth was to be located.

In addition, a point was selected on each azimuth between 20 and 80 nm by sequentially selecting additional random numbers from the table (rejecting those numbers less than 20 or greater than 80) and assigning the numbers as ranges on the various azimuths.

Along each selected azimuth on each selected photograph, the distance to, and path length through, any precipitation was tabulated. In addition, a YES or NO was recorded as to whether there was precipitation over the ten selected points.

A total of 139 photographs were examined; thus, data were recorded for 1390 azimuths. These data were used as estimates of l, the path length through convective precipitation. Figure 6 shows a PPI photograph of shower precipitation, together with the selected azimuths and points.

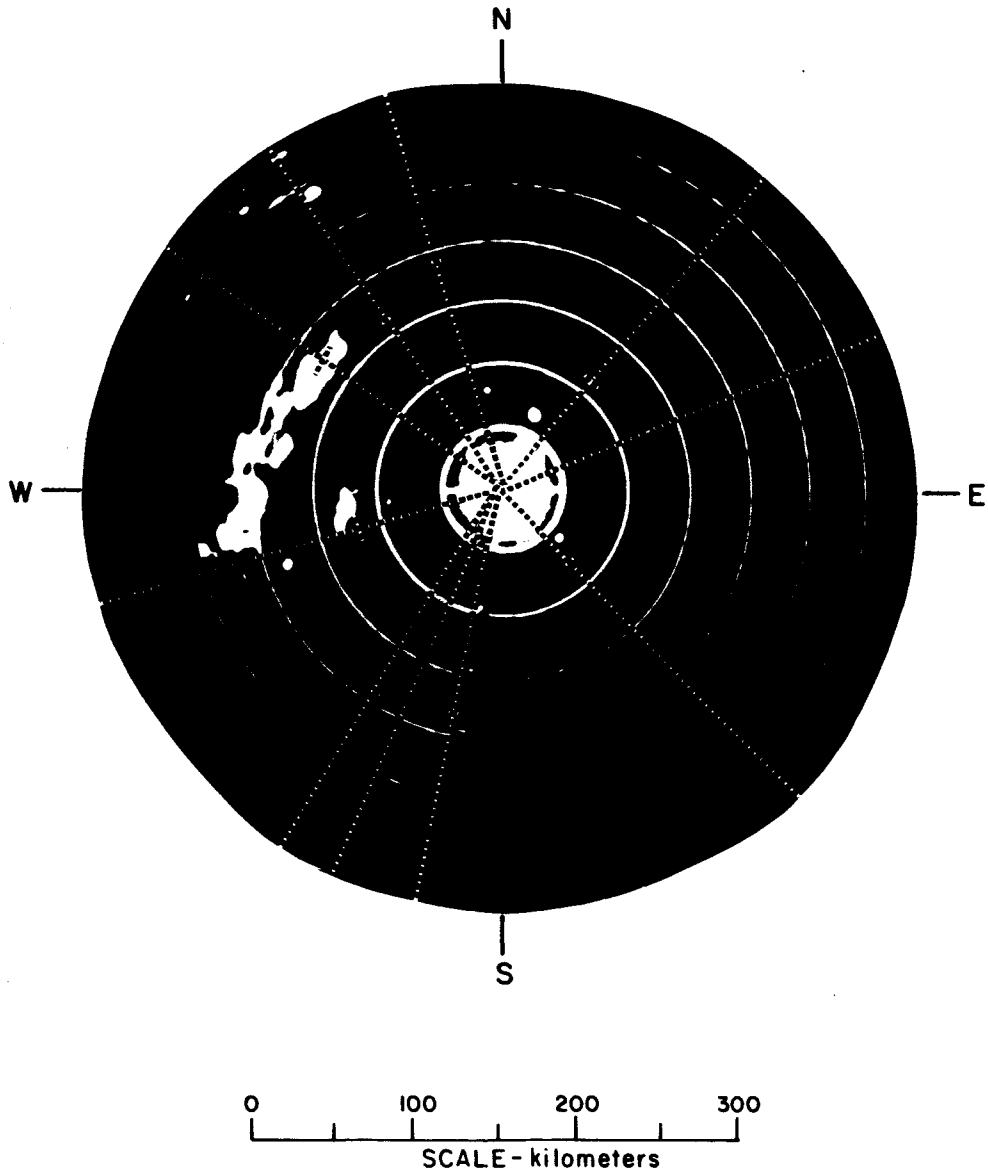

FIG. 6 PPI PHOTOGRAPH OF RADAR-DETECTED CONVECTIVE PRECIPITATION

The total time there was precipitation over a point, or within an area surrounding the point, was estimated by combining the point data from Portland, Maine, with the areal radar data. The Portland data provided the duration of both continuous and shower-type precipitation at the site. The radar data provided knowledge of the frequency with which there was a shower over a specific point when there were showers in an area. These two bits of knowledge on showers can be combined by writing

$$\frac{T_s}{T} = \frac{\frac{T_{sp}}{T}}{\frac{T_{sp}}{T_s}}$$

where

T_s = time showers occur

T = total time

T_{sp} = time there are showers at a point.

The numerator T_{sp}/T is evaluated from the Portland point data by dividing the duration of showers by the length of record examined. The denominator T_{sp}/T_s is determined from the radar by evaluating the ratio of the number of times a point on the radarscope photograph had echo to the total number of points on the radarscope photographs that were examined.

As numerical examples:

$$\frac{T_{sp}}{T} = \frac{8953}{223,200} = 0.041$$

$$\frac{T_{sp}}{T_s} = \frac{165}{1390} = 0.119$$

$$\frac{T_s}{T} = \frac{0.041}{0.119} = 0.345 \quad .$$

Thus, while there are showers over the point 4.1 percent of the time, there are showers within interfering range 34.5 percent of the time.

III PROBABILITY DISTRIBUTIONS OF INTERFERENCE TEMPERATURE

A. INTRODUCTION

Based on the scattering cross-section models and data on the frequency of occurrence of various types and rates of precipitation, probability distributions of interference temperature were calculated by a B 5500 computer. The computations were made for the months of January (winter); April (spring); July (summer); and October (fall). For each month, the day was divided into four time periods, in addition to the computation for the entire day. The times of day that were examined were the periods containing the hours ending 01 to 06, 07 to 12, 13 to 18, and 19 to 24 EST. For each month and each time period, computations were made both when the interfering signal was present at all levels and when it was only present above altitudes of 2, 4, 6, 7, 8, 9, 10, 11, 12, 13, 14 km. In addition, computations were made for an antenna pointing at the zenith as well as 10 degrees above the horizon. Additional angles of 2.5 and 5 degrees above the horizon were also computed for July.

The calculated values of interference temperature for all the combinations of conditions mentioned above were obtained from the computer, expressed as the percent of time the interference temperature was greater than 10^{0}, 10^{1}, ..., 10^{6} K. Plotted curves of these data are shown in Figs. 7 to 10. The figures also contain a curve of estimated probability distributions of sky temperatures. These sky temperatures are discussed in Sec. IV of the report.

B. VARIATIONS IN INTERFERENCE TEMPERATURES

1. Variations Due to Height of Interfering Signal and Elevation Angle

Figure 7 shows the probability distribution of interference temperature for winter (January). During this month an interfering signal extending to the surface will result in an interference temperature in excess of 10^{0} K some 12 percent of the time (see Fig. 7a).

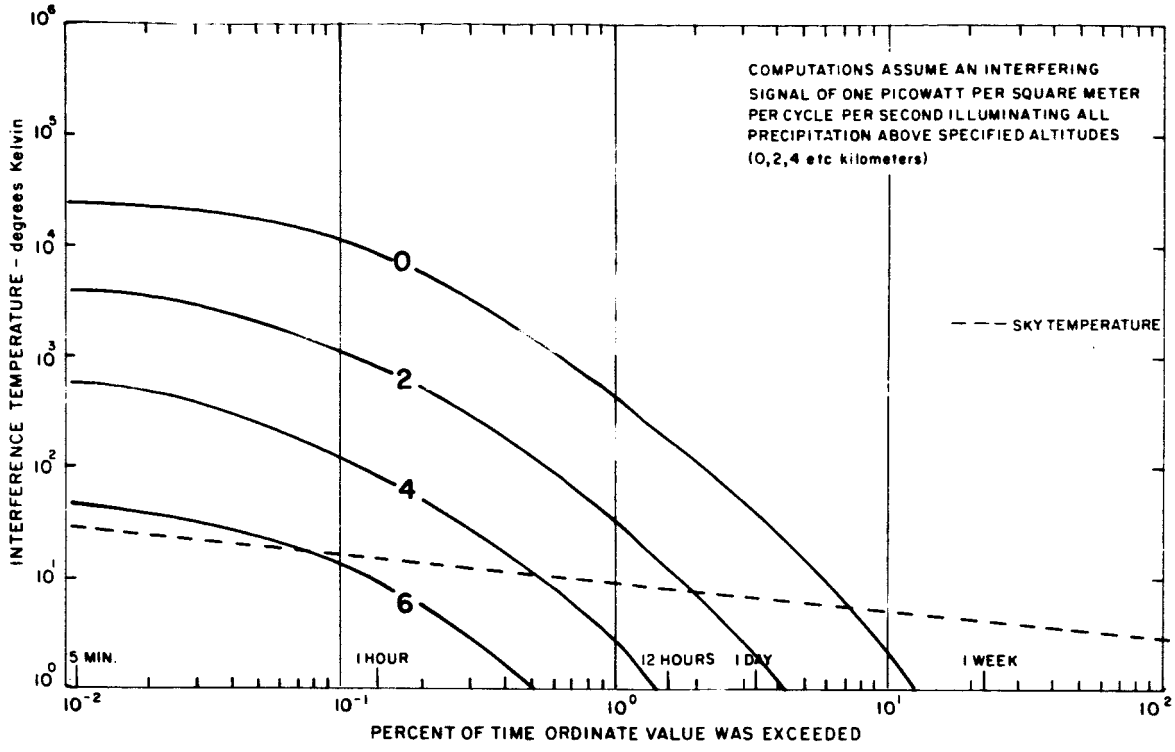

(a) ANTENNA POINTED AT ZENITH

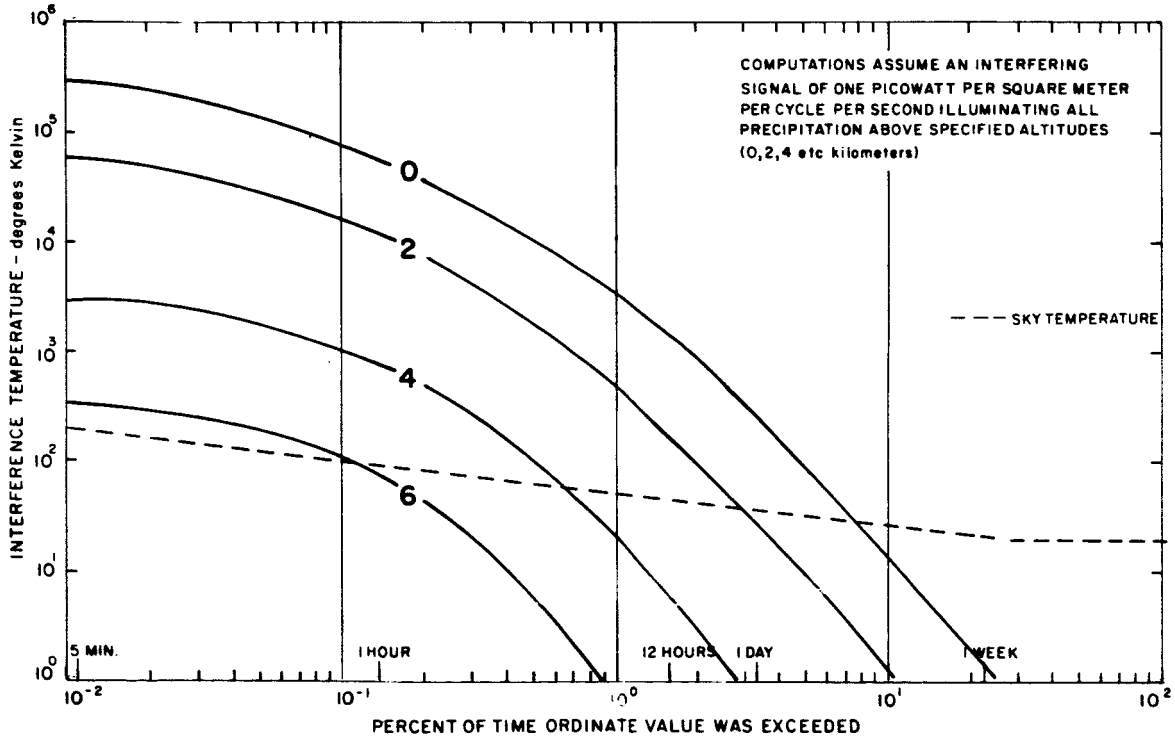

(b) ANTENNA POINTED TEN DEGREES ABOVE HORIZON

FIG. 7 PROBABILITY DISTRIBUTION OF INTERFERENCE TEMPERATURES AT PORTLAND, MAINE, IN JANUARY

Approximately one hour per month, a vertically pointing antenna will experience an interference temperature of 10^4 K. When the interfering signal is only present above 6 km, the comparative values drop to a value of 10^0 K one-half of one percent of the time, and the interference temperature exceeded one hour per month is reduced to 10^1 K. When the antenna elevation is 10 degrees above the horizon (Fig. 7b), interference temperatures are approximately one order of magnitude higher for any given percent of the time. There is still no measurable interference temperature when the interference source is above 6 km, since the mean height of the melting level is below the surface (surface temperature below freezing), and the rates of precipitation are relatively low. Thus, the portion of Fig. 3 that is important in computing interference temperatures is in the upper left, i.e., above the melting level and with precipitation rates at the lower end of the indicated values.

Figure 8 shows probability distributions of interference temperature for spring (April). In Fig. 8a, where it is assumed that the antenna is pointed at the zenith, interference temperatures will exceed 10^0 K about 12 percent of the time, and a value 10^4 K will be exceeded about one hour per month. During this month, there is a potential interference temperature of 10^0 K less than one hour per month when the interfering source is above 8 km.

With the antenna pointed 10 degrees above the horizon, all interference temperatures are again about one order of magnitude greater for any given percent of the time when the interfering signal extends to low levels. At this angle the path length through the lighter precipitation at higher levels is sufficient for interference a larger percent of the time, even when the interfering source is about 8 km.

Figure 9 shows probability distributions of interference temperature during summer (July). Figure 9a, for the antenna at the zenith, shows an interference temperature of 10^0 K about 8 percent of the time when the interfering signal is down to the surface; and with the same level of interference, the figure shows an interference temperature of 10^4 K, 6×10^{-1} percent of the time. The curves for interfering signal

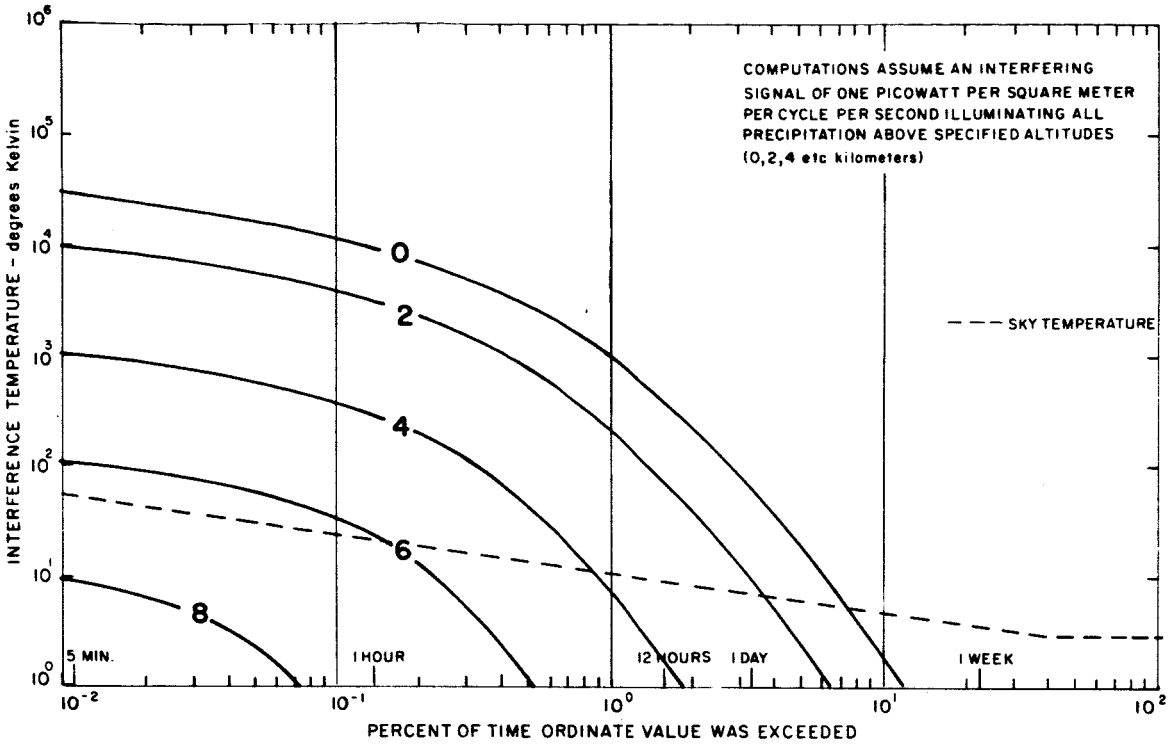

(a) ANTENNA POINTED AT ZENITH

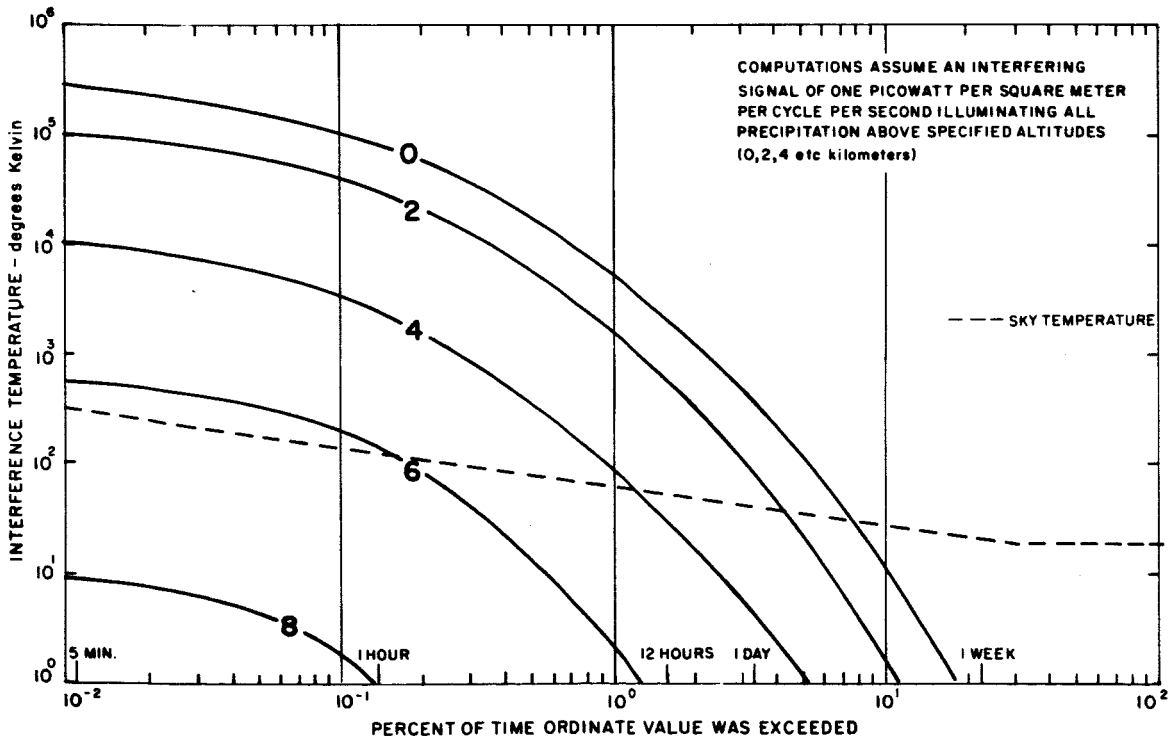

(b) ANTENNA POINTED TEN DEGREES ABOVE HORIZON

FIG. 8 PROBABILITY DISTRIBUTION OF INTERFERENCE TEMPERATURES AT PORTLAND, MAINE, IN APRIL

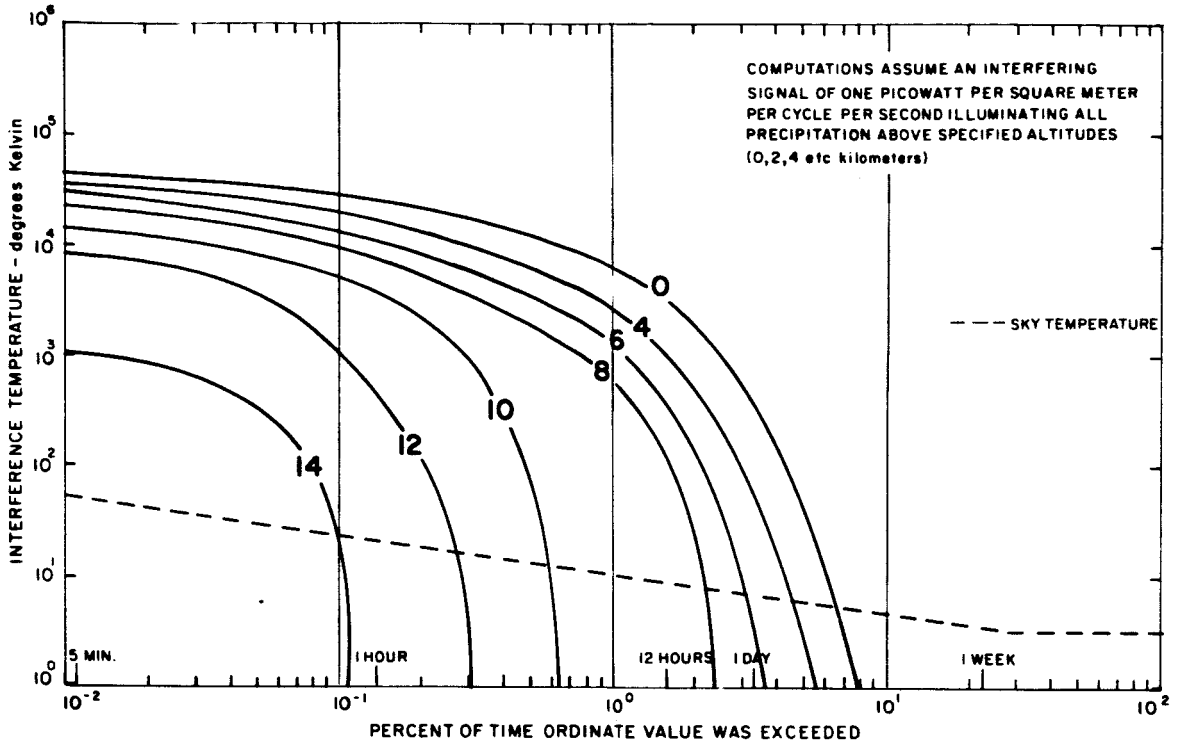

(a) ANTENNA POINTED AT ZENITH

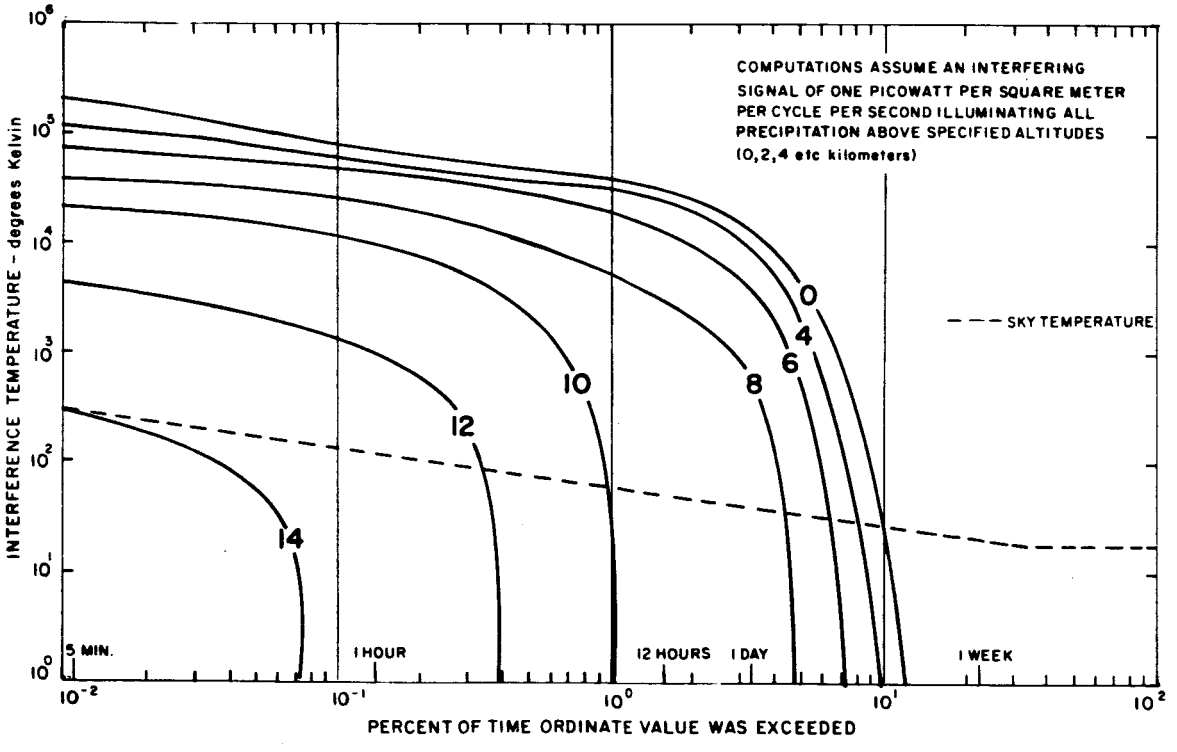

(b) ANTENNA POINTED TEN DEGREES ABOVE HORIZON

FIG. 9 PROBABILITY DISTRIBUTION OF INTERFERENCE TEMPERATURES AT PORTLAND, MAINE, IN JULY

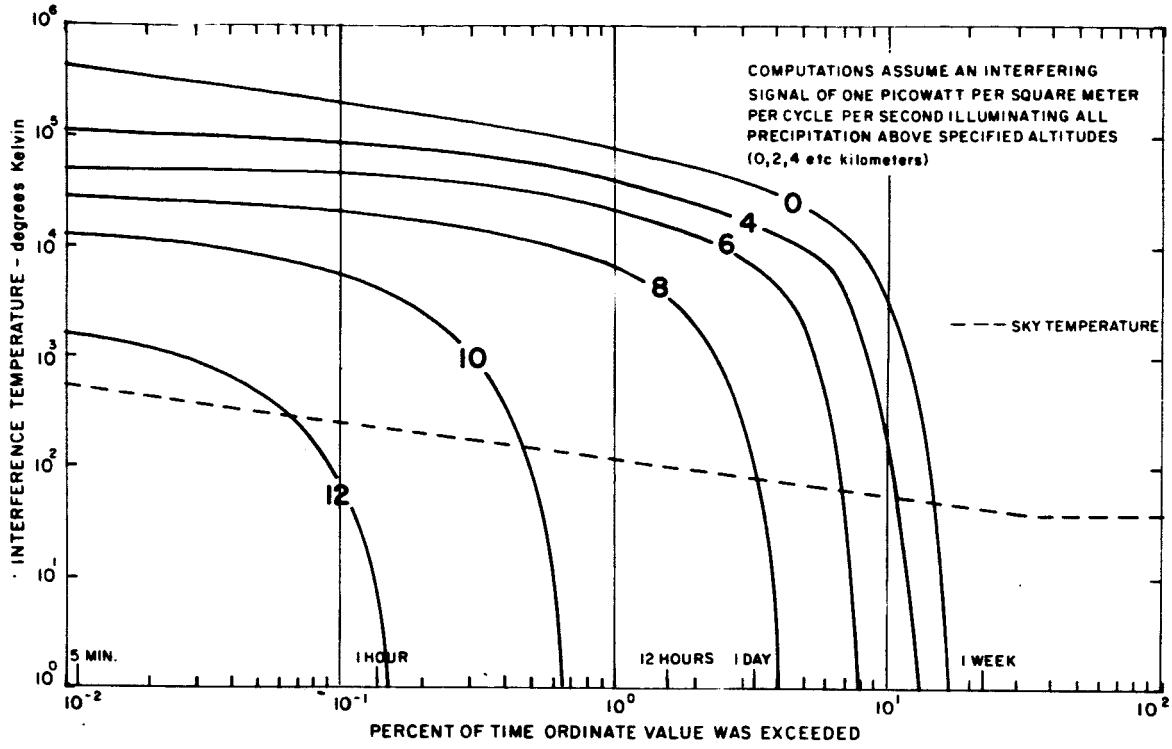

(c) ANTENNA POINTED 5 DEGREES ABOVE HORIZON

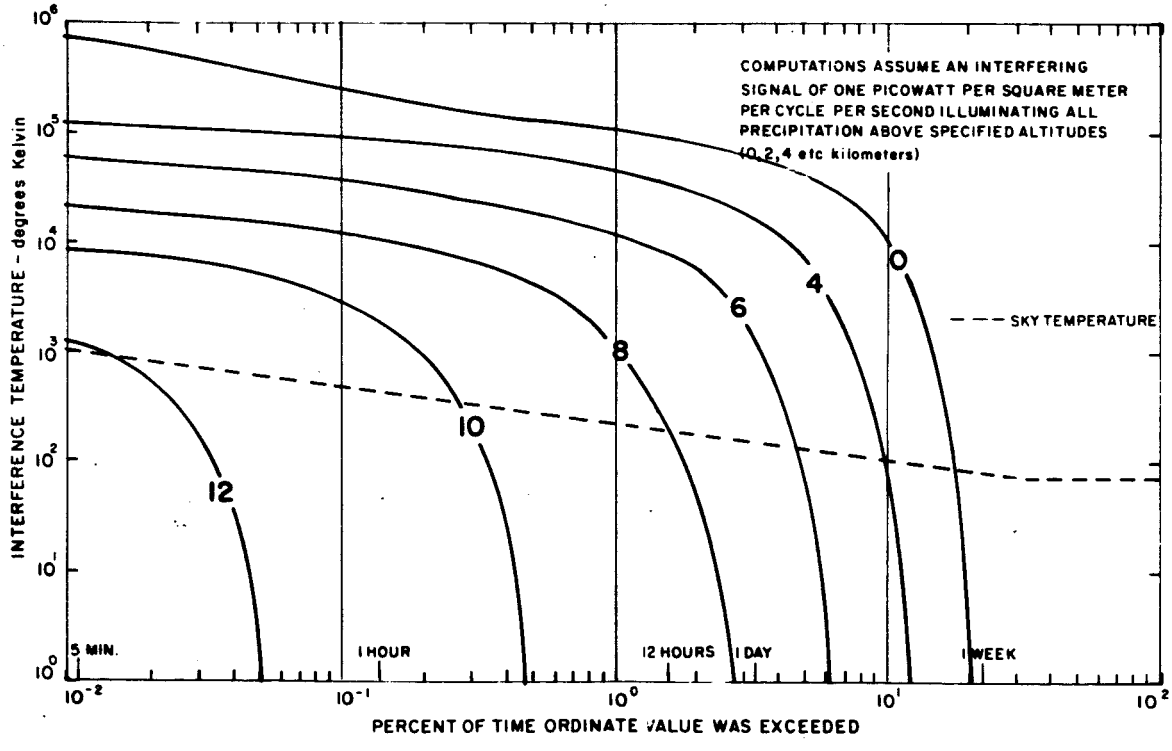

(d) ANTENNA POINTED 2.5 DEGREES ABOVE HORIZON

FIG. 9 (Concluded)

at various levels are quite closely spaced, especially for small percentages of the time, and show that interference temperatures of 10^3 K could be experienced even when the interfering signal is above 14 km.

With the antenna aimed 10 degrees above the horizon, the probability distribution is somewhat different than with the antenna at the zenith. The percent of time the interference temperature will exceed 10^0 K is increased to 12 percent when the interfering source is at the surface; but the spacing between curves for different altitudes of interfering signal becomes greater, so that the percent of time there will be measurable interference above 14 km and the magnitude of this interference is decreased.

With an antenna elevation of 5 degrees above the horizon (Fig. 9c), the percent of time the interference temperature exceed 10^0 K increases to 17 percent (when h = 0) and the maximum values of interference temperature increase, but the level above which the interference temperature could be computed drops to 12 km. In the curves for an elevation angle of 2.5 degrees above the horizon (Fig. 9d), there is a further increase in the percent of time that the interference temperature exceeds 1 K and also an increase in maximum interference temperature (to almost 10^6 K), but the percent of time and maximum value of interference temperature when the interfering signal is above 12 km is lower than that shown by Fig. 9c. The shapes of these July curves are due to the predominence of showers extending to relatively high altitudes. They imply that when the interfering signal is present at relatively low levels (say, less than 6 km), the interference temperature will be quite high; that is, it will exceed 10^4 K nearly as frequently as it will exceed 10^0 K. This causes the curves to rise very steeply. The changes in the curves as the elevation angle is varied toward the horizon is due in part to interception of more of the convective cells at long ranges, which increases the maximum interference temperatures and increases the percent of time a given interference temperature will be exceeded, and in part to the fact that when an interfering signal is present only above high altitudes (say, 12 km), the antenna beam through a shower may be

well below that level, causing a decrease in the maximum interference temperatures computed for the interfering signal above selected levels only.

Figure 10a shows probability distributions of interference temperature with the antenna pointed at the zenith in October. When the interfering source extends to the surface, an interference temperature of 10^0K is exceeded 15 percent of the time. Maximum illustrated values are close to 10^5 K. The precipitation extends to sufficiently high altitudes during this month to produce significant interference temperatures, even when the interfering signal is above 8 km.

When the antenna elevation is 10 degrees above the horizon (Fig. 10b), the interference temperatures for any given percent of the time are one order of magnitude greater than when the antenna is pointed at the zenith. The close spacing of the curves for an interfering signal altitude of 0 and 2 km is a reflection of the fact that the bright band is generally above 2 km, and therefore, according to Fig. 4, there would be little difference between the two levels.

2. Variations with Season and Time of Day

Differences of interference temperatures among the four seasons, illustrated in Figs. 7 to 10, should be related to differences in the vertical extent, type, and intensity of precipitation during the four seasons. To facilitate a comparison, data from the four months were replotted to show the comparative interference temperature exceeded (when the interfering source is above various levels) for various percentages of time. Figure 11 shows the interference temperature exceeded one day per month for each season. This curve was constructed by examination of Figs. 7 to 10 and by replotting from each figure the value of interference temperature at the percent of time corresponding to one day. The figure shows that there is an increase in interference temperature during the warmer part of the year. This increase is even more pronounced at an antenna elevation of 10 degrees above the horizon. The effect of the greater vertical extent of summertime precipitation is especially noticeable from a comparison of interfering signals above various levels. In

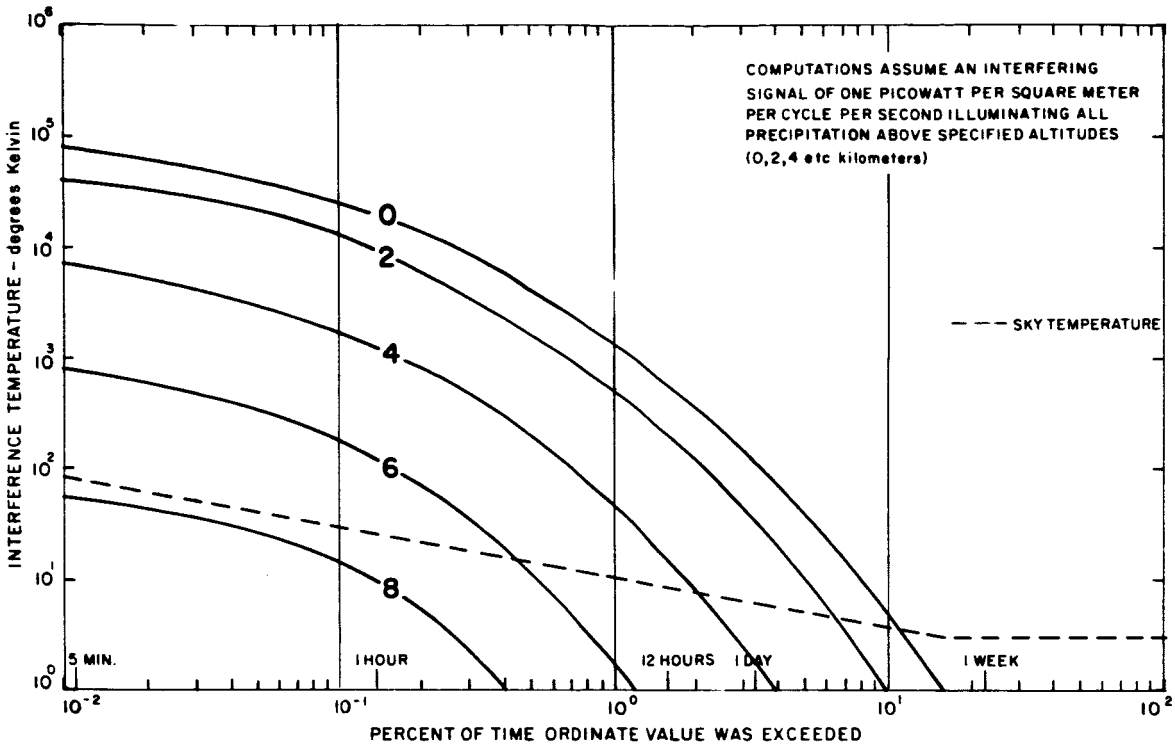

(a) ANTENNA POINTED AT ZENITH

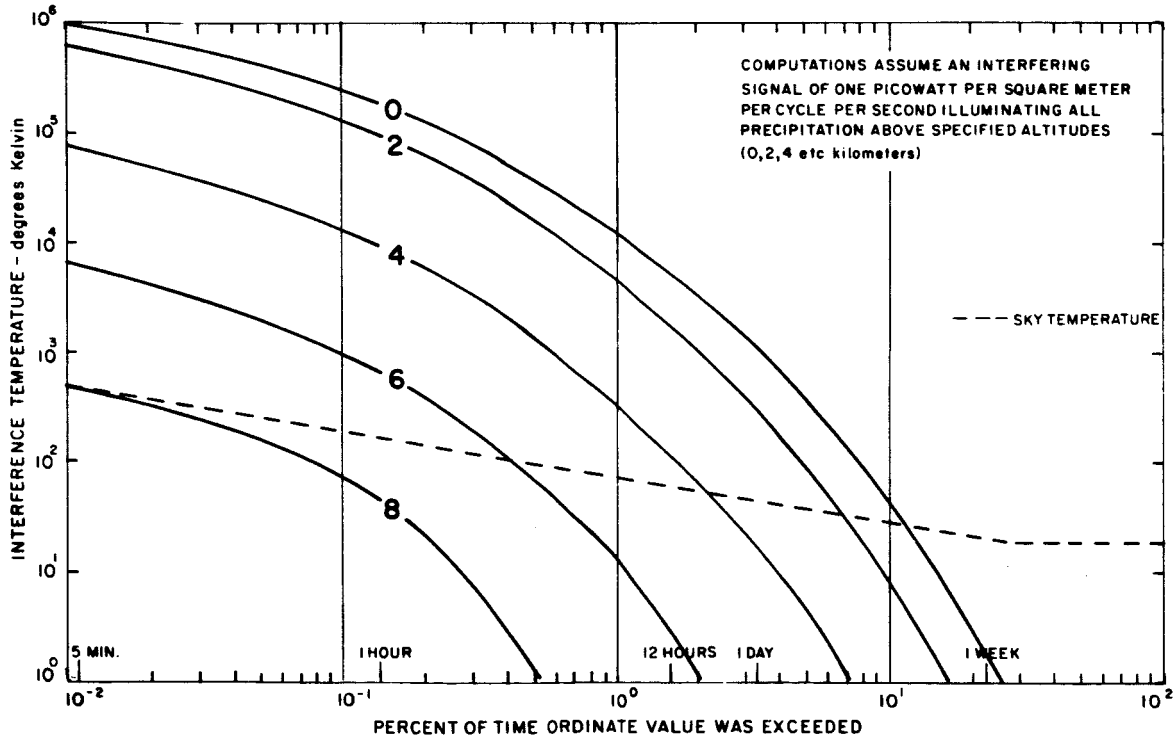

(b) ANTENNA POINTED TEN DEGREES ABOVE HORIZON

FIG. 10 PROBABILITY DISTRIBUTION OF INTERFERENCE TEMPERATURES AT PORTLAND, MAINE, IN OCTOBER

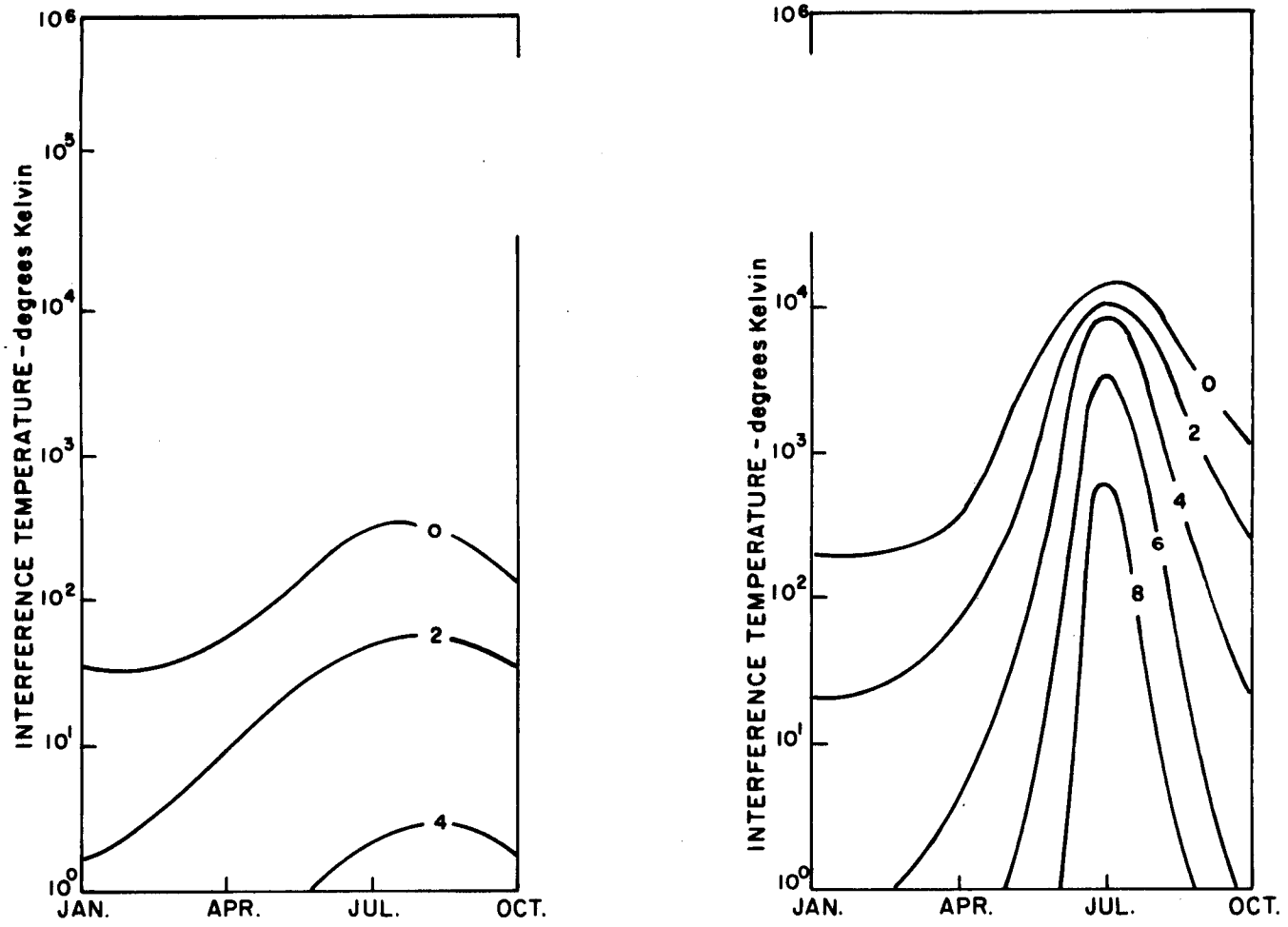

FIG. 11 INTERFERENCE TEMPERATURE EXCEEDED ONE DAY PER MONTH

Fig. 11b, for example, when the interfering signal present is only above 4 km, the resulting interference temperatures are relatively low--except in July, when they are comparable to those obtained when the interfering signal extends to the surface.

When one considers the seasonal variations of interference temperatures exceeded one hour per month (Fig. 12a), the picture changes somewhat. The seasonal difference in maximum interference temperature is less, but July still has much higher values when the interfering signal is restircted to higher levels. At an elevation angle of 10 degrees (Fig. 12b), the maximum interference temperature, when the interfering signal extends to the surface, is comparable to that of January but is lower than that of April and October. The effect of showers extending to high altitudes in July is, however, still present, as shown by measureable interference temperatures when the interfering source is 12 km above the surface.

An examination of interference temperatures exceeded 5 minutes per month (Fig. 13) shows that October has the highest values when the interfering signal is within 2 km of the surface; but when the signal is higher, the greater vertical extent of July precipitation makes July the month of maximum interference temperatures.

These figures demonstrate the importance of summertime convective activity. Although there are fewer minutes of precipitation during July than during the other months, the vastly greater vertical extent and locally greater intensity results in much higher interference temperatures, when the interfering source is at relatively high levels.

The variations with time of day would also be greatest during the summertime, since the convective activity varies markedly with surface heating by solar radiation. The time of maximum heating is shortly after local noon, and there is an additional one- or two-hour lag before convective storms reach maximum intensity. Although the data sample considered in this study proved rather small for the plotting of curves of significant differences between the four time periods of the day, some conclusions can be drawn from distributions of precipitation rates. An

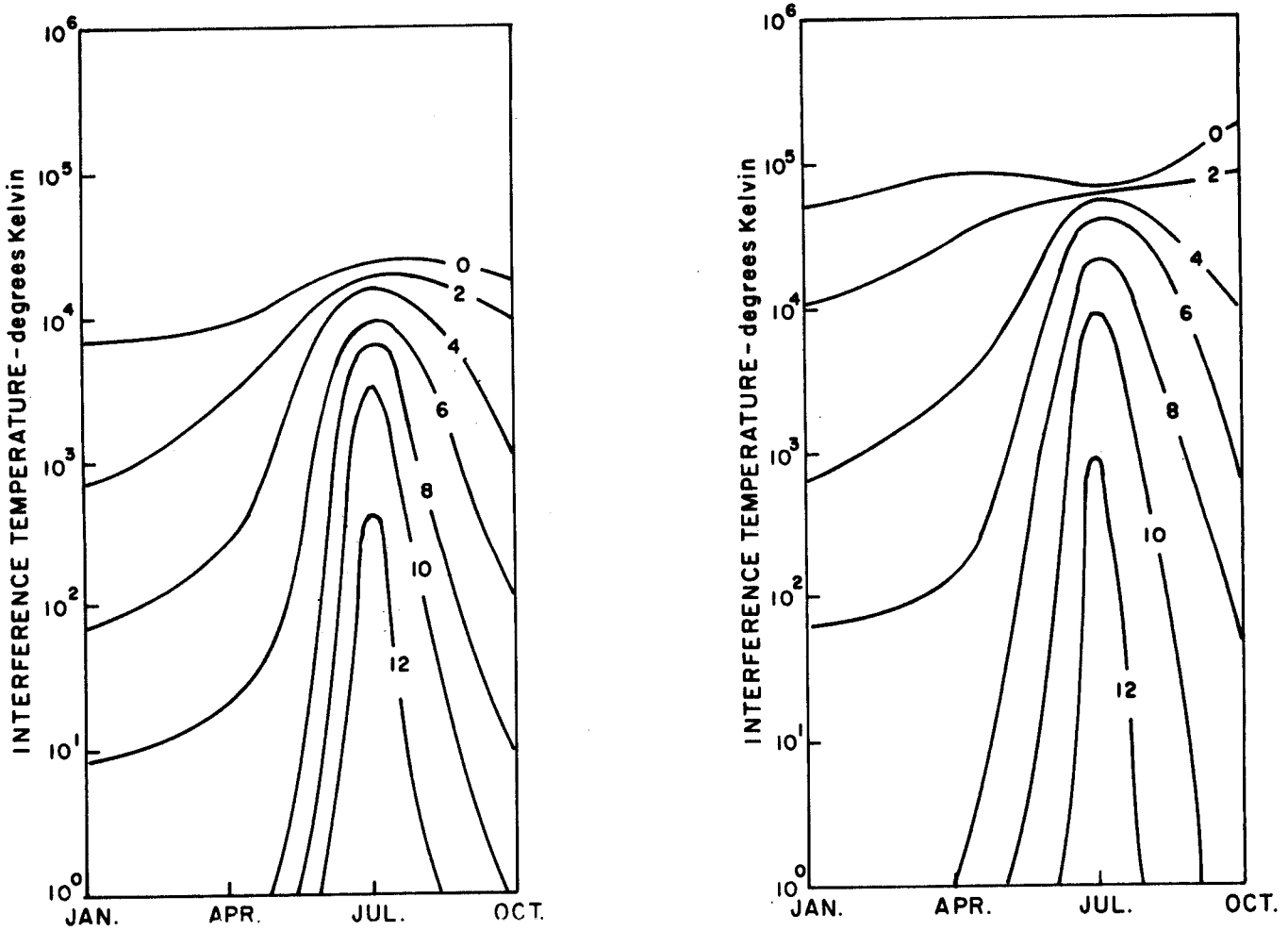

FIG. 12 INTERFERENCE TEMPERATURE EXCEEDED ONE HOUR PER MONTH

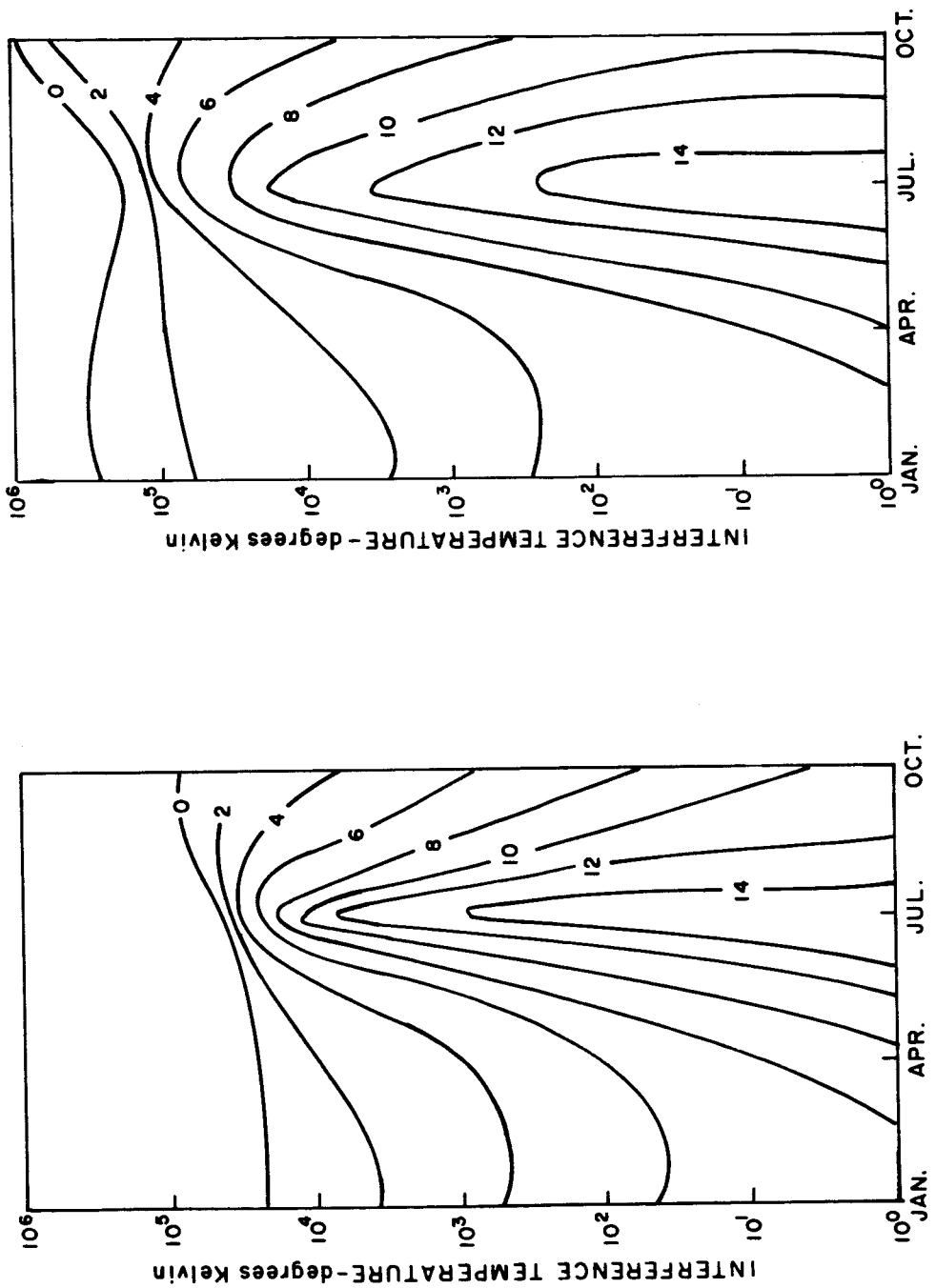

FIG. 13 INTERFERENCE TEMPERATURE EXCEEDED FIVE MINUTES PER MONTH

examination of cumulative distributions of rainfall rates at Portland, Maine,[12] for the period 1951 to 1960 shows that the relative frequencies of rain rates varied with season and time of day, as shown in Table II.

Table II

NUMBER OF HOURS IN 30 MONTHS THAT PRECIPITATION RATE EXCEEDED 6.4 mm/hr^{-1}

	Time of Day			
Season	01-06	07-12	13-18	19-24
Winter	12	10	5	3
Spring	2	13	15	18
Summer	7	14	23	16
Fall	12	19	21	20

The table shows a tendency for more hours of high rates during the period 0100 to 1200 EST in winter. During the spring and fall, there is not much change during the period 0700 to 2400. In the summer there is a definite maximum during the period 1300 to 1800 EST. The effect of these variations would be to cause differences in the percent of time a given interference temperature was exceeded during the different periods of the day. The shapes of the curves would probably not change; instead, they would merely slide back and forth along the x-axis.

IV COMPARISON OF INTERFERENCE TEMPERATURES AND SKY TEMPERATURES

A. DISCUSSION OF SKY TEMPERATURES

Hogg and Semplak[13] made measurements of sky temperatures both during periods of clear weather and during periods of rain. They found that there was no one-to-one comparison between surface rainfall rate and sky temperature, but they emphasize that the rainfall rates were measured only at the antenna site, while the sky noise is the integrated result of an extended path through the atmosphere. There are many possible reasons why Hogg and Semplak found no direct correlation between rainfall rate at the antenna site and sky noise (although several of their figures show a very strong tendency of the two parameters toward the same direction). One is storage of rainfall in the cloud owing to strong updrafts, another is shear of the rain column, and a third is a time lag between rain aloft and the collection of water in the rain gauge. (The last effect is mentioned in Sec. II B of this report in connection with correlation of radar reflectivity aloft and surface rainfall rates.)

For lack of any better data then those given by Hogg and Semplak, it has been assumed that there is some loose correlation between surface rainfall rate and sky temperature. This relationship can be derived from Fig. 13 of Ref. 13 and is presented here as Fig. 14, which compares sky temperature with instantaneous rainfall rates. The rainfall rates for a long-term period at Portland, Maine, are for hourly periods. However, Bussy[14] gives a relationship between instantaneous rates and those for other intervals. Using Bussey's curve, the 10-year average rainfall data for Portland were converted to instantaneous rates, and from Fig. 14 the sky temperature corresponding to this rate was determined. These values of sky temperature were plotted on Figs. 7, 8, 9, and 10 at the percent of time corresponding to the percent of time the rainfall rates would occur. To extrapolate, from the zenith to other elevation angles, it was assumed that the trend would be the same as that shown by Fig. 5 in Ref. 13, i.e., the path length was the most important parameter in increasing the temperature as the antenna elevation approached the horizon.

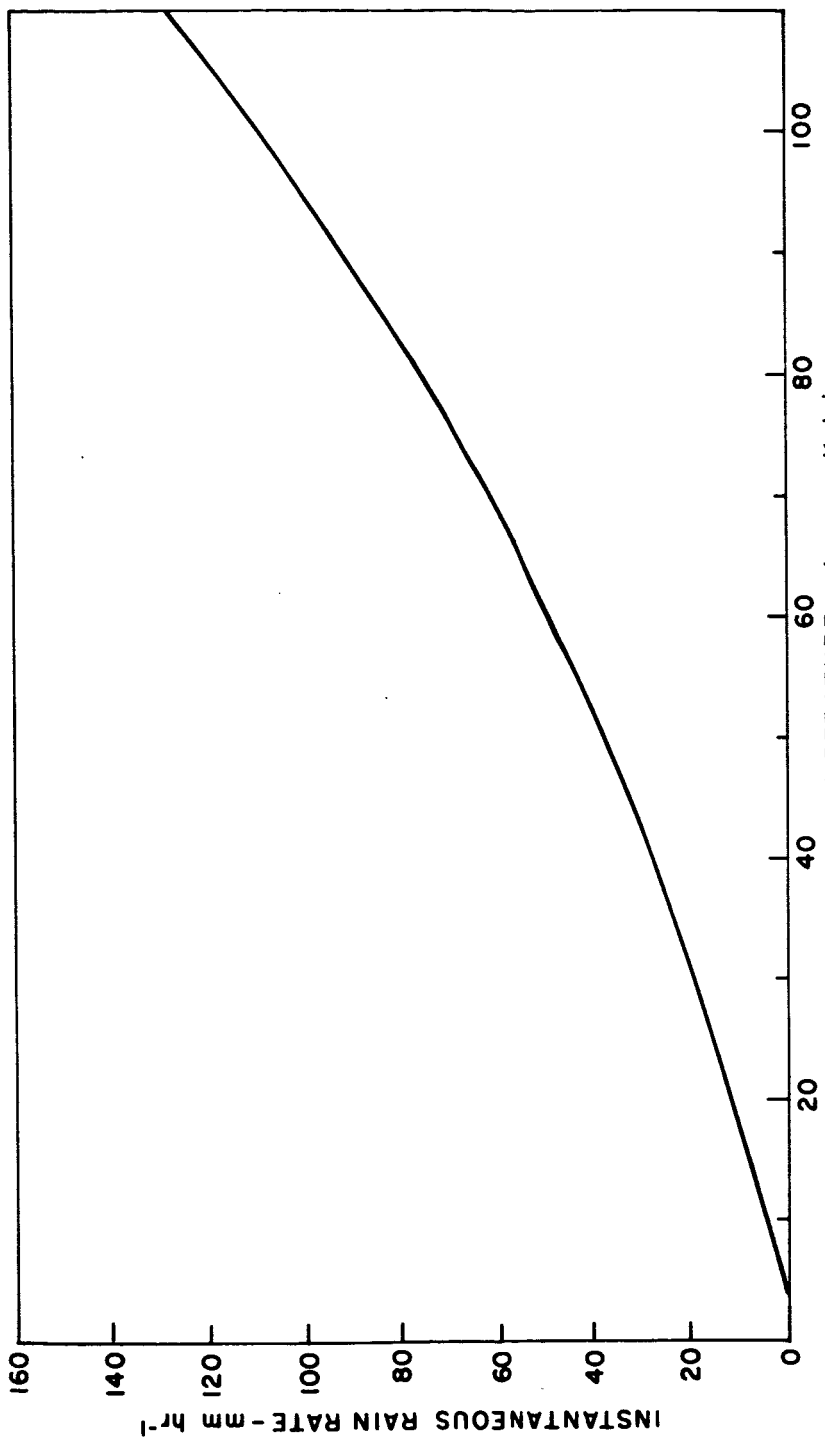

FIG. 14 ASSUMED RELATIONSHIP BETWEEN INSTANTANEOUS RAINFALL RATE AND ZENITH SKY TEMPERATURE

The sky temperatures shown on Figs. 7, 8, 9, and 10 are at best, therefore, only ball park estimates, but they do serve for comparison with magnitudes of interference temperature. The sky-temperature values at the right-hand side of the figures, representing those obtained when there is no precipitation, are reasonably well accepted. It is only the shape of the curve and the maximum value experienced for very short time periods that are in question. Whether 1000 K at a 2-1/2-degree elevation angle for about 5 minutes a month in July (Fig. 9d) is overly optimistic or pessimistic can only be answered by actual measurements taken during some 20 Julys. During all seasons, a no-rain sky temperature of 3 K at the zemith was assumed. This also probably varies a few degrees, but in comparison with interference temperatures which increase to 10^4 K or more, the difference between sky temperatures of say 2 K and 5 K seems negligible.

B. RELATIVE MAGNITUDES OF INTERFERENCE AND SKY TEMPERATURES

Figures 7, 8, 9, and 10 show probability distributions of interference temperatures when an interfering source of one picowatt per square meter per cycle per second illuminates the common volume above various selected altitudes and also shows an estimate of the probably sky temperatures. The figures all show that a large percentage of the time, at least three weeks out of the month, the sky temperatures will exceed interference temperatures. The remaining seven days of each month, conditions change very rapidly, since during these seven days rain of varying intensities and varying vertical extent occurs. Examination of the figures shows that to keep the maximum interference temperature at least equal to the sky temperature, the interfering signal must be above 6 km in January and April, above 12 to 15 km in July, and above 8 km in October. The figures show the percent of time that the sky temperature is equal to the interference temperature when the interfering signal is present above various altitudes. Since the curves of interference temperature slope much more than those of sky temperature, the level above which the interfering signal is present is the major contributor to the percent of time a given temperature will be exceeded.

In July, for example, when the interference temperature curves are closely spaced, the difference between the time the sky temperature is equal to the interference temperature, when the interfering signal is at the ground and at 8 km, is only 4 percent of the time, or 30 hours. During other months there is a drastic difference if there is only 2 or 4 km difference in the level above which the interfering signal is present. For example, in January the difference of 2 km above the surface in the altitude of the interfering signal means that the time during which the interference temperature will equal the sky temperature is decreased by 58 hours.

V PREDICTION OF INTERFERENCE TEMPERATURES AT OTHER LOCATIONS

A. INTRODUCTION

Previous sections of this report have shown that the basic parameters important in producing large interference temperatures are frequent and intense precipitation extending to high altitudes and a source on interfering radiation that illuminates this precipitation. As estimate of the probability distribution of interference temperature at any other location, as compared with that for New England, must, therefore, consider how the distribution of precipitation at the other location compares with that at Portland. A comprehensive analysis of the differences between Portland and other areas in probable interference temperatures must consider the relative vertical extent, intensity, and seasonal and diurnal variations. These meteorological parameters must then be interpreted in terms of the physical and electrical parameters of potential sites.

B. METEOROLOGICAL PARAMETERS

1. Seasonal Distribution of Precipitation

The globe is divided into a number of precipitation regimes. Some of these regimes have specific boundaries, owing to topographical features. Other regimes have no specific boundaries; instead, there is a zone of transition across which thr precipitation distribution changes. Many of these precipitation distributions may be illustrated by stations in various sections of the United States. Figure 15 shows the variability of monthly precipitation at selected stations. Data for this figure are from World Weather Records,[15] except the data for Portland, Maine, which was taken from the 1941 Yearbook of Agriculture.[16] The figure shows considerable variability, both from north to south and from east to west, in monthly precipitation amount and season of maximum or minimum precipitation. At Portland the monthly totals are comparatively uniform throughout the year, although there is a tendency toward larger values in the winter and spring. Southward along the east coast there is an increasing trend toward greater precipitation amounts during the warmer months and less precipitation during

the colder months. This seasonal effect is even more pronounced over the north central part of the country, where there is a well-marked summer maximum precipitation and relatively little wintertime precipitation. Over the Rocky Mountain states, between about 110 and 115 degrees West longitude, there is very little precipitation during any month, with a tendency toward higher monthly totals during the colder half year. Along the Pacific Coast there is a very well-marked wet winter season and a dry summer season. In addition, there is an increase in maximum wintertime monthly totals from south to north.

The totals shown on Fig. 15 are long-period means, and any specific year could depart markedly from the mean. At San Francisco, for example, where the mean December rainfall is 104 mm, there was a range during the period 1951 to 1960 from a minimum of 10 mm in 1953 to a maximum of 312 mm in 1955. An accurate prediction of the probability distribution at any location would require a long-range prediction of probable precipitation during the period under consideration. The longer the period, the more closely conditions would approach the mean; but then for any given year, predicted distributions of interference temperatures could be vastly different from observed conditions.

2. Precipitation Intensity

While mean monthly rainfall totals give a measure of probable interference temperature, the intensity at which the precipitation occurs must be considered, since this is related to maximum values of interference temperature. The only method of constructing probability distributions of precipitation intensities at a given location would be to analyze data collected at or near the specific site in question. Without, however, analyzing precipitation intensity data at a number of locations, it is possible to draw some conclusions about rain rates by considering the type of precipitation that is most frequent in various parts of the country. There is a seasonal variation in precipitation intensity as well as in total precipitation. In areas where a considerable proportion of the wintertime precipitation falls as snow, the precipitation rates could be much lower than those associated with rain.

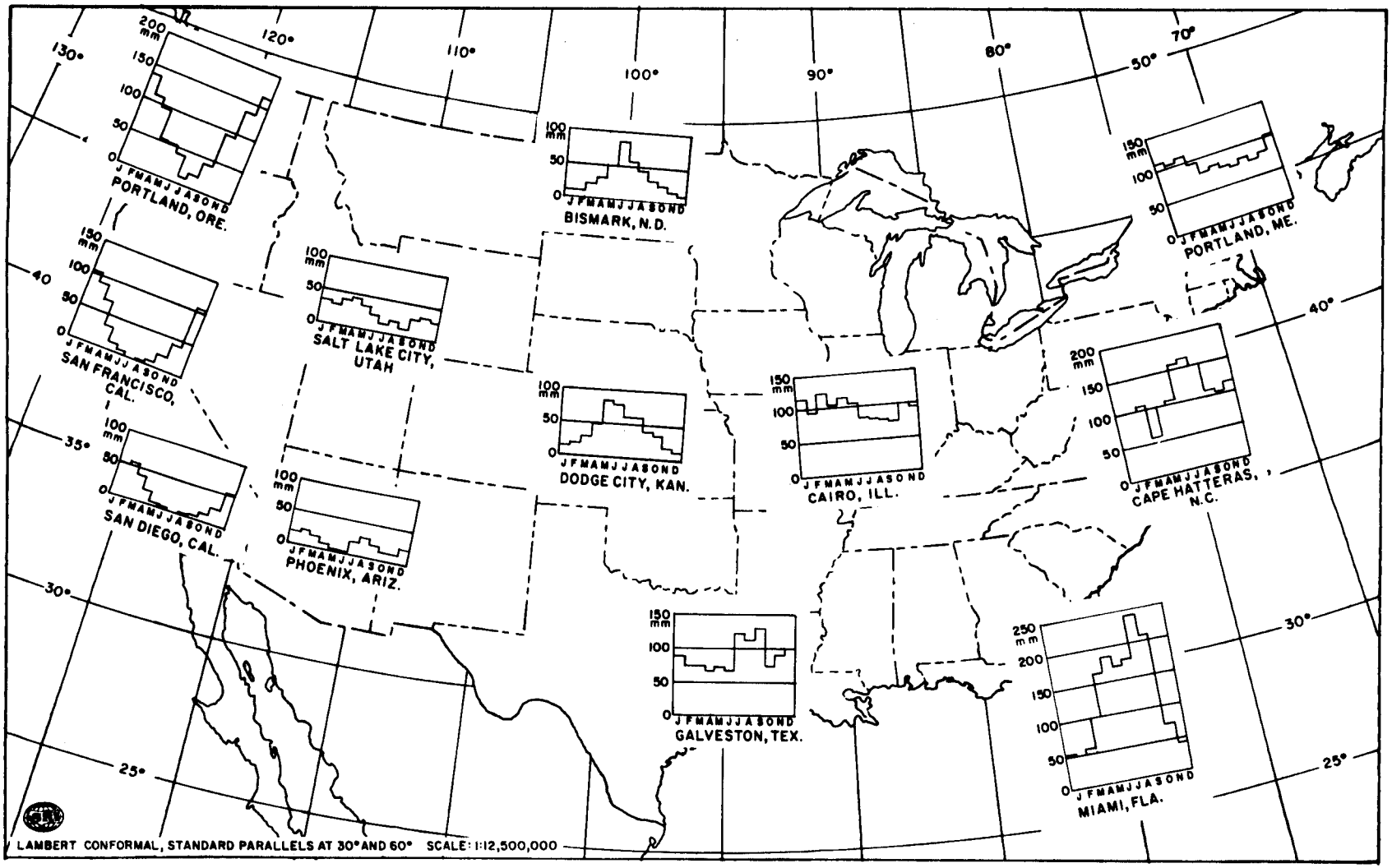

FIG. 15 VARIABILITY OF MONTHLY PRECIPITATION

For example, Cole and Donaldson[17] plotted the ratio of annual precipitation divided by the number of days with 0.25 mm or more precipitation against the percentage of time precipitation rates of 1.5, 3.0, and 4.5 mm per hour were equaled or exceeded and found correlation coefficients of 0.878, 0.955, and 0.960, respectively. They further found that 99 or more percent of all precipitation rates equal to or exceeding 3.0 mm per hour occurred only with temperatures above freezing. About 85 percent of the rates half as great also occurred with temperatures above freezing.

Their studies may be interpreted to mean that in areas with little precipitation and where the wintertime precipitation falls as snow, and hence at low rates, there would be a low probability of significant interference temperatures. As examples, Salt Lake City, Utah, and Bismark, North Dakota, both have low wintertime precipitation, according to Fig. 15. Visher[18] shows that 30 percent of the annual precipitation at these locations falls as snow. Therefore, these locations would have very negligible interference temperatures during the colder months. In other areas, notably the coastal regions of the United States, an insignificant fraction of the annual precipitation falls as snow.

The precipitation which does not fall as snow, and hence can be assumed to have somewhat higher rates and therefore higher interference temperatures, may be classified into two types: (1) the relatively uniform continuous precipitation associated with major storm systems, most frequent during the fall, winter, and spring; and (2) the convective precipitation during the summer. The rates at which the continuous precipitation occurs in any given location are probably quite similar to those at Portland, Maine, during October, and the major difference in probability distributions of interference temperature between Portland and another location would be due to the frequency of occurrence of continuous precipitation. In areas of greater total monthly rainfall, there would be curves of similar shapes but with a shift toward a higher percent of the time. In areas of lower monthly precipitation, the curves of interference temperature would be shifted toward a lower percent of the time. There could also be some minor differences in the magnitudes

of interference temperatures above various levels, but these would be minor compared to the summertime convective precipitation.

The intensity of summertime convective precipitation is closely related to the vertical extent of the precipitation. The vertical extent of the more severe convective activity, hence highest rainfall rates, can be compared at various locations by considering the height of the tropopause. The tropopause used to be regarded as an upper limit to convection, since above this level the atmosphere becomes warmer with increasing altitude, and rising parcels of air penetrating this layer would become colder than their environment, thus losing their buoyancy and ability to rise further.

Recent studies[9,10] have shown that more violent thunderstorms penetrate the tropopause to varying degrees, depending on location, season, and time of day. One study[9] gives heights of the tropopause and the number of thunderstorms that penetrated the tropopause by 1.5 and 3.0 km. An adaptation of these values of average tropopause heights and the number and percent of thunderstorms that exceeded the tropopause height is given in Table III.

In Ref. 9, the authors explain that the great majority of these tropopause penetrations are during the summer months and during the time of day from 1200 to 2000, with the major peak between 1600 and 1700 LST.

In the above-referenced study, the station closest in space and climatic regime to Portland, Maine, is New York City. At that station some tops penetrated 3 km or more above the 12-km tropopause. At more southerly stations, notably New Orleans, a substantial number of tops penetrated to 3 km or more above a 14-km tropopause, or to 17 km or more.

A more recent report[10] does not give average tropopause heights but does give the average yearly tropopause penetrations during the period 1961 through 1964. These values have been combined with data on the average tropopause heights from Ref. 9 to give an estimate of the relative numbers of thunderstorm tops extending to various altitudes at various locations. Table IV shows the combined data from Refs. 9 and 10.

Table III

TROPOPAUSE HEIGHT AND PENETRATIONS BY THUNDERSTORMS AT SELECTED STATIONS

Station	Average Tropopause (km)	Number and Percent of Penetrations above 1.5 km		3.0 km	
Amarilo, Texas	13	50	8.3	17	7.9
Tampa, Florida	14	59	9.8	9	4.2
New Orleans, Louisiana	14	212	35.3	73	34.0
Missoula, Montana	11	16	2.7	1	0.5
Kansas City, Missouri	12	175	29.2	90	41.8
Brownsville, Texas	15	12	2.0	5	2.3
New York, New York	12	58	9.7	19	8.8
Wilmington, Delaware	13	8	1.3	0	0
Sacramento, California	12	10	1.7	1	0.5

Table IV

AVERAGE ANNUAL NUMBER OF THUNDERSTORM TOPS EXTENDING TO VARIOUS ALTITUDES

Station	Altitude (km)								
	12	13	14	15	16	17	18	19	20
Amarillo, Texas			74	67	32	17	12	1	0*
Tampa, Florida				36	52	12	1		
New Orleans, Louisiana				316	281	146	84	26	9
Missoula, Montana	27	15	1						
Kansas City, Missouri			506	220	118	64	41	11	1
Brownsville, Texas					10	28	10	4	1
New York City		106	52	21	3				
Wilmington, Delaware			10	3	0	0	0		
Sacramento, California		13	4						

*1 or 2 during the four-year period.

It should be strongly emphasized that the implied heights in this table are subject to many uncertainties. For example, the maximum tropopause penetration may have occurred when the tropopause was at a height much lower than average. The table is presented merely as a possible guide to maximum convective heights in various regions of the United States; the available radar records have not been summarized in the form of the number of tops at various heights above sea level.

Table IV implies that tops do not exceed 21 km and that generally the lower tops are over the western part of the United States. The general inference of this table is consistent with other evidence that relates thunderstorm severity to thunderstorm height; i.e., areas such as Amarillo, Texas, and Kansas City, Missouri, have more violent storms (more hail and tornadoes) than New York City or Missoula, Montana. For planning potential precipitation scatter interference during summer months, therefore, it would be relevant to consider the possibility of occasional convective activity to at least the altitudes suggested by Table IV.

The model of backscatter cross section given in Sec. II-C for convective precipitation should apply to convective activity in all locations. Therefore, when the precipitation extends to very great altitudes, the interference temperatures should be very large if an interfering source is present down to the surface at the receiver site, and substantial interference temperatures should be experienced, even if the interfering signal is present only above relatively high altitudes.

C. SITE PARAMETERS

The discussion of precipitation in the preceding sections shows that potential satellite ground stations in many climatological areas must be located such that any interfering signal is only present above rather high altitudes. Sites located where there is little annual precipitation, and where much of the precipitation occurs as snow, can tolerate much lower altitudes of interfering signal than sites located in areas of considerable summertime convective precipitation. An

example of the former is a station located in the northern Rocky Mountain states, where monthly precipitation totals rarely exceed 50 mm and almost one third of the annual precipitation falls as snow. An example of the latter is a Gulf Coast station, where summertime precipitation may exceed 200 mm per month and where this rainfall occurs in thunderstorms extending above 20 kilometers. It appears therefore, that areas of the United States that have the greatest convective precipitation and also the most frequent and intense continuous precipitation are those areas that have the flattest terrain, and therefore, terrain shielding of a receiver site from potential interference sources is practically impossible. In addition, many of the areas of maximum rainfall are areas of greater population density, greater industrial activity, and more numerous emitters of electromagnetic radiation. The selection of a site or sites that would be remote from interfering sources and would have little precipitation scatter from these remote interference sources thus tends to center on some desert region or on some low rainfall region such as that found in the Rocky Mountain states. In this region, precipitation is at a minimum. At the more northerly latitudes, about one third of the precipitation occurs as snow, and the mountainous terrain could offer shielding from potential interference sources.

VI RECOMMENDATIONS FOR FUTURE WORK

Many aspects of the determination of probability distribution of precipitation scatter interference are somewhat indefinite because of lack of available data or because study of all available data did not fall within the scope of the research reported herein. The readily available surface observations of rainfall give the percent of time the rainfall rate exceeds 7.6 mm hr^{-1} but do not give the maximum rates that may occur. Thus, the maximum interference temperatures that might occur could not be determined.

Many assumptions were made in deriving the models of backscattering cross sections of the continuous and convective precipitation. Although these models were based on available information in published literature, there is much additional information that has not been analyzed and published. For instance, many radar sites routinely photograph RHI scopes, and thus there exist films showing the vertical extent of radar-detectable precipitation. Except for cases of severe weather causing major loss of property and life, these data have not been summarized and published.

More recent advances in the state of the art in radar data collection provide three-dimensional intensity contours of precipitation. These, as a significant sample becomes available from various sites, would provide needed knowledge of three-dimensional probability distributions of precipitation intensity.

Future work on the problem of precipitation scatter interference could be divided into three types of studies. First, a number of the older radar records could be collected and examined to determine more precisely the probability distributions of the maximum vertical extent of radar-detectable precipitation at a number of locations. Second, the more recent quantitative radar films could be collected and analyzed to refine intensity distributions of precipitation at various altitudes. The results of these studies could be strongly biased, depending upon

whether this more sophisticated equipment were operated routinely or were used only to collect data on cases of the more severe weather, such as hail, tornadoes, flash floods, and hurricanes.

Finally, a program could be initiated specifically to collect data on the frequency with which interference temperatures of various magnitudes were encountered. Such a program would take considerable time and require a number of receivers at various distances from a given interference source, or a number of pairs of receivers and interference sources. Concurrent with the collection of such data, there should be three-dimensional quantitative radar records (possibly the radar could serve as the interference source) as well as the conventional rainfall and radiosonde data that the weather bureau has collected for many years. By simultaneously collecting interference temperature data and three-dimensional rainfall data, some of the assumptions that were necessary in this report could be eliminated.

A comparison of the three courses of action outlined above would suggest that to gain additional information most rapidly, the best procedure would be to collect all available quantitative radar data (both PPI and RHI) that have been collected with increasing frequency during the past few years for a number of selected sites (such as Champaign, Illinois; Cambridge, Massachusetts; Miami, Florida; College Station, Texas; Corvallis, Oregon; Seattle, Washington; McGill University, Montreal, Canada) and for a number of USWB WSR-57 sites, and make the best possible climatological assessment of the probability distribution of horizontal and vertical precipitation intensity profiles. While such a program would not be inexpensive (due to cost of film reproduction) and would require considerable time to analyze the large sample data involved, it would provide very worthwhile knowledge of the vertical distribution of precipitation.

REFERENCES

1. Dennis, A. S., "Forward Scatter from Precipitation as an Interference Source at Stations Monitoring Satellites," Research Memorandum 2, Contract NASr-49(02), SRI Project 3773, Stanford Research Institute, Menlo Park, California (November 1961, revised).

2. Dennis, A. S., "The Scattering of SHF Radio Waves by Hail and Wet Snow," Final Report, Contract NASr-49(02), SRI Project 3773, Stanford Research Institute, Menlo Park, California (June 1964).

3. Culnan, D. E., F. O. Guiraud, and R. E. Skerjanec, "Radio Scattering Cross Sections of Thunderstorms," NBS Report 8816, U.S. Department of Commerce, National Bureau of Standards, Boulder Laboratories, Boulder, Colorado (June 1965).

4. Wexler, R., and P. M. Austin, "Radar Signal Intensity from Different Levels in Steady Snow,: Research Report No. 23, Contract No. DA-36-039 SC-42625, Massachusetts Institute of Technology, Cambridge, Massachusetts (1954).

5. Dennis, A. S., "Measurements of Forward Scatter from Rain at 9.05 Gc," Research Memorandum 4, Contract NASr-49(02), SRI Project 3773, Stanford Research Institute, Menlo Park, C lifornia (1962).

6. Austin, P. M., "Radar Measurements of Precipitation Data," Proceedings of the 1964 World Conference on Radio Meteorology Incorporating the Eleventh Weather Radar Conference, pp. 120-125 (1964).

7. Fernald, F. G., and A. S. Dennis, "Measurement of Forward-Scatter Cross Sections in the Melting Layer," Proceedings of the 1964 World Conference on Radio Meteorology Incorporating the Eleventh Weather Radar Conference, pp. 178-181 (1964).

8. Byers, H. R., and R. R. Braham, Jr., The Thunderstorm (U.S. Government Printing Office, Washington, D.C., 1949).

9. Hanks, H. H. Jr., M. J. Long, and R. G. Beebe, "Tropopause Penetrations by Cumulonimbus Clouds," Scientific Report 1, AFCRL-64-111, Contract AF 19(628)-2454, Atmospheric Research and Development Corporation, Kansas City Missouri (February 1964).

10. Long, M. J., "Tropopause Penetrations by Cumulonimbus Clouds-II," Scientific Report 2, AFCRL-65-331, Contract AF 19(628)-2454, Atmospheric Research and Development Corporation, Kansas City, Missouri (April 1965).

11. Dennis, A. S., "Rainfall Determinations by Meteorological Satellite Radar," Final Report, Contract NASr-49(06), SRI Project 4080, Stanford Research Institute, Menlo Park, California (April 1963).

12. U.S. Department of Commerce, Climatography of the United States, No. 82-17, Decennial Census of U.S. Climate--Summary of Hourly Observations, Portland, Maine 1951-1960 (U.S. Government Printing Office, Washington, D.C., 1963).

13. Hogg, D. C., and R. A. Semplak, "Effect of Rain and Water Vapor on Sky Noise at Centimeter Wavelengths," Bell System Tech. J., Vol. 40, pp. 1331-1348 (September 1961).

14. Bussey, H. E., "Microwave Attenuation Statistics Estimated form Rainfall and Water Vapor Statistics," Proc. IRE, Vol. 38, No. 7, pp. 781-785 (July 1950).

15. U.S. Department of Commerce, World Weather Records 1951 to 1960, Vol. 1, North America (U.S. Government Printing Office, Washington, D.C., 1965).

16. U.S. Department of Agricultute, Climate and Man, 1941 Yearbook of Agriculture (U.S. Government Printing Office, Washington, D.C., 1941).

17. Cole, A. E., and R. J. Donaldson, "Precipitation, Clouds, and Aerosols," Sec. 5.1 of Handbook of Geophysics and Space Environment, S. L. Valley, ed. (McGraw Hill Book Co., Inc., 1965).

18. Visher, S. F., Climatic Atlas of the United States (Harvard University Press, 1954).

ACKNOWLEDGMENTS

The research described in this report was performed in the Aerophysics Laboratory under the direction of Dr. M. G. H. Ligda, Laboratory Manager, and the immediate supervision of Mr. R. T. H. Collis, Head of the Laboratory's Radar Aerophysics Group. In addition to the guidance and supervision of Dr. Ligda and Mr. Collis, the assistance given by the following individuals is gratefully acknowledged.

Dr. A. S. Dennis developed the concept of precipitation scatter interference as an interference temperature. Mr. F. E. Fernald, Research Meteorologist, searched the literature for pertinent data on profiles of vertical distribution of precipitation and reduced published information to workable models. Mr. John E. Alder, Research Meteorologist, extracted and summarized surface observations of precipitation for computer processing. Mr. R. Yaeger, Statistician, devised the methods of selection and analysis of radarscope photographs. Messrs. R. Robinson and M. I. Smith, Meteorological Assistants, performed the task of tabulating the necessary data from the radarscope photographs. Mr. R. L. Mancuso, Research Meteorologist, wrote the computer programs required to calculate interference temperatures from the models and observational data.

Appendix

COMPUTATION OF INTERFERENCE TEMPERATURES FROM CONVECTIVE PRECIPITATION

The data from which interference temperatures for convective showers were determined consists of the distance to and path length through radar echoes located along ten randomly selected azimuths (see Sec. II C 2). The geometry of the computations, with showers of various sizes at various distances, is shown by Fig. A-1. On this figure the symbols have the following meaning:

θ = elevation angle

D = distance to shower

L = horizontal path length through the shower

H = height of the shower

h = height at which the antenna beam intercepts the center of the shower

$\mathcal{J}$ = level above which an interference source is present

G = range at which the beam penetrates the base of the region illuminated by an interference source.

The length of the horizontal path through the echo, L, is assumed to be equivalent to the shower diameter. Then, as outlined in Fig. 4, the height of the shower H is related to L as follows:

$$L \leq 14.8 \text{ km}, \quad H = L$$

$$14.8 < L \leq 20.3 \text{ km}, \quad H = 29.3 - L$$

$$L > 20.3 \text{ km}, \quad H = 9.3 \text{ km}.$$

With the large areas of convective activity at long ranges, it is likely that the beam will penetrate the top of the shower and that the

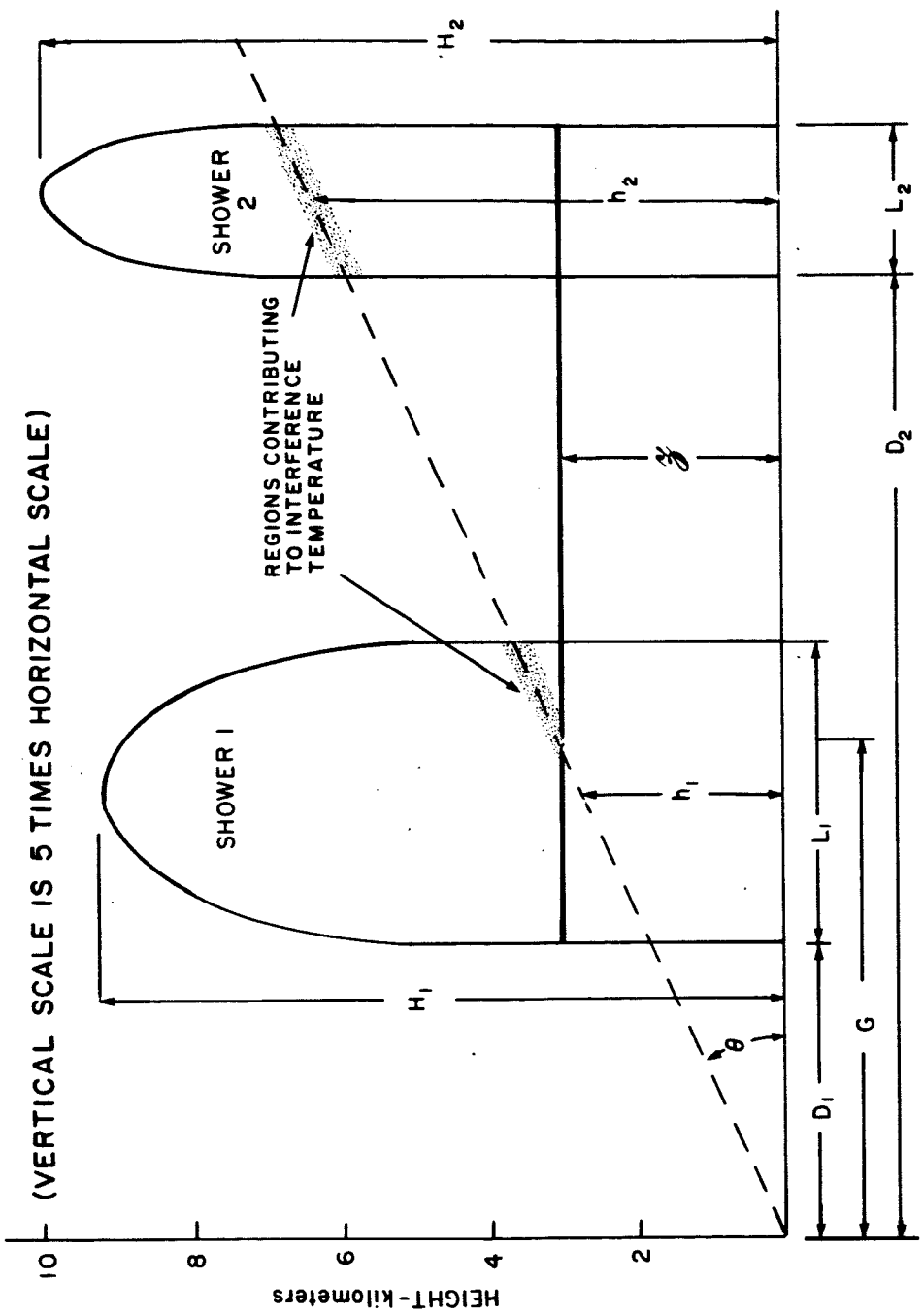

FIG. A-1 GEOMETRY OF COMPUTATION OF INTERFERENCE TEMPERATURES FROM SHOWERS
(See text for definitions of symbols.)

value of L will overestimate the length of the contributing path through the storm. For cases of $L > 20.3$ km, a computation was made using the equation

$$L' = -D + ka \tan \theta + \sqrt{(D + ka \tan \theta)^2 - 2\, ka\, (D \tan \theta - 9.3)} \qquad \text{(A-1)}$$

where

L' is effective horizontal path length

ka is effective earth radius.

If L' was smaller than L, it was used in subsequent calculations.

The height at which the antenna beam intersects the core of the shower is given by

$$h = \left(\frac{L}{2} + D\right) \tan \theta + \frac{\left(D + \frac{L}{2}\right)^2}{2\, ka} \qquad \text{(A-2)}$$

where the last term is a correction for the earth's curvature, with the 4/3 earth approximation of ka = 8500 km.

When the level of the interfering signal is above the surface, it is possible for the beam to be within a shower but wholly or partially below the level that could contribute to interference temperature. Therefore, it is necessary to consider the range G at which the beam begins to penetrate the base of the region illuminated by the interfering source. Range G is related to $\mathcal{Z}$ (the altitude above which interference is present) by the equation

$$G = -8500 \tan \theta + \sqrt{(8500 \tan \theta)^2 + 17000\, \mathcal{Z}} \quad . \qquad \text{(A-3)}$$

The calculations of interference temperature for showers are just extropolations of the basic expression Eq. (10):

$$T_i = 4.05\, H^{2.5}\, L \quad ,$$

which gives the interference temperature under conditions where

$$G \leq D \text{ and } h \leq \frac{H}{2} \quad ,$$

that is, where the entire path within the shower is illuminated by the interference source and the beam is penetrating the lower half of the shower.

Under conditions wherein $G \leq D$ but the beam is in the dome of the model shower, i.e., $\frac{H}{2} < h \leq H$, it can be shown that the basic expression must be modified and becomes

$$T_i = 4.05\ H^{2.5}\ L \times F\left(\frac{2h - H}{H}\right) \quad , \tag{A-4}$$

where

$$F\left(\frac{2h - H}{H}\right) = \int_{\frac{2h-H}{H}}^{1} \frac{\alpha\ (1 - \alpha)^{2.5}}{\sqrt{\alpha^2 - \left(\frac{2h - H}{H}\right)^2}}\, d\alpha \quad . \tag{A-5}$$

and α is a dimensionless parameter describing the location of the point of integration.

In all cases where $h > H$, the beam is assumed to completely overshoot the shower, and T_i is then zero.

If $D < G < D + L$, then only a portion of the path through the shower is illuminated, and by setting new limits of integration on Eq. (8) for the cases where $h < \frac{H}{2}$ and $L \leq 20.3$ km,

$$T_i = 4.05\ H^{2.5}\ L \times \frac{1}{2}\left[1 + \frac{D + \frac{L}{2} - G}{\left|D + \frac{L}{2} - G\right|}\left(1 - \left\{1 + \frac{2}{L}\left|D + \frac{L}{2} - G\right|\right\}^{35}\right)\right] \quad . \tag{A-6}$$

For simplicity, cases with $L < 20.3$ km are assumed to be single showers, and on that basis the added factor has been applied to the basic interference temperature expression Eq. (A-4). For the larger values of L, it is likely that more than one shower lies along the beam. Therefore, the more sophisticated assumptions of Eq. (A-6) are not justified, and

the following simple extrapolation of Eq. (10) is used for $D < G < D + L$, $h \leq \frac{H}{2}$, and $L > 20.3$ km:

$$T_i = 4.05\ H^{2.5}\ L \times \frac{D + L - G}{L} \quad . \qquad \text{(A-7)}$$

For simplicity, with $D < G < D + L$ and $\frac{H}{2} < h < H$, t_i was taken as the above expression corrected by the factor $F\left(\frac{2h - H}{H}\right)$:

$$T_i = 4.05\ H^{2.5}\ L \times \frac{D + L - G}{L}\ F\left(\frac{2h - H}{H}\right) \quad . \qquad \text{(A-8)}$$

For $D + L < G$, the beam will be under the illuminated region of the shower, and $T_i = 0$.

From the radar films it was impossible to separate showers over the station from near-field clutter. To approximate T_i for showers over the station, then, a point along each of the azimuths used was selected to represent the station. When radar detected showers were over this point, an interference temperature representing conditions with showers over the station could be calculated. For low elevation angles, this was simply performed by using the above equations, but in every case the distance D of the equations was replaced by D - X, where X is the range to the point selected to represent the station.

For showers over the station and an antenna elevation angle of 90 degrees, the following modification to the basic equation results if $\mathcal{g} \leq \frac{H}{2}$:

$$T_i = 34\ H^{3.5} \times \frac{1}{2}\left[3.5\left(1 - \frac{|2D + L - 2X|}{L}\right)^{2.5}\left(1 - \frac{2\mathcal{g}}{H}\right) + F\left(\frac{|2D + L - 2X|}{L}\right)\right] .$$

The first term within the brackets is the factor derived for the path within the cylindrical portion of the shower, and $F\left(\frac{|2D + L - 2X|}{L}\right)$ is the factor for the portion of the path through the dome of the shower and is the same as Eq. (A-3) but with differently defined limits of integration. The value of interference temperature contributed by only

a fraction of the dome when $\frac{H}{2} < \mathcal{J} < H$ was roughly approximated as shown below:

$$T_i = 34H^{3.5} \times \frac{1}{2}\left[1 - \left(\frac{2\mathcal{J}}{H} - 1\right)^{3.5}\right]\left[F\left(\frac{|2D - L - 2X|}{L}\right)\right]$$

STANFORD RESEARCH INSTITUTE

Menlo Park
California

Regional Offices and Laboratories

Southern California Laboratories
820 Mission Street
South Pasadena, California 91031

Washington Office
1000 Connecticut Avenue, N.W.
Washington, D.C. 20036

New York Office
270 Park Avenue
New York, New York 10017

Detroit Office
1025 East Maple Road
Birmingham, Michigan 48011

Chicago Office
103 S. Stone Avenue
La Grange, Illinois 60525

Huntsville, Alabama
4810 Bradford Drive, N.W.
Huntsville, Alabama 35805

European Office
Pelikanstrasse 37
Zurich 1, Switzerland

Japan Office
Nomura Securities Building
1–1 Nihonbashidori, Chuo-ku
Tokyo, Japan

Retained Representatives

Toronto, Ontario, Canada
Cyril A. Ing
86 Overlea Boulevard
Toronto 17, Ontario, Canada

Milan, Italy
Lorenzo Franceschini
Via Macedonio Melloni, 49
Milan, Italy

Printed in U.S.A. January 1966